FRONT MATTER

TITLE

UBA1-depleted neutrophils disrupt immune homeostasis and induce VEXAS-like autoinflammatory disease in mice

Authors

Ge Dong[1,2,3,#], Jingjing Liu[1,2,3,#], Wenyan Jin[1,2,3,Δ], Hongxi Zhou[1,2,3,Δ], Yuchen Wen[1,2,3,Δ], Zhiqin Wang[1,2,3,Δ], Keyao Xia[1,2,3], Jianlin Zhang[1,2,4], Linxiang Ma[1,2,3], Yunxi Ma[1,2,4], Lorie Chen Cai[3], Qiufan Zhou[5], Huaquan Wang[5], Wei Wei[6], Ying Fu[7], Zhigang Cai[1,2,3,4,5,6,*]

Affiliations

[1]Tianjin Key Laboratory of Inflammatory Biology, Department of Pharmacology, School of Basic Medical Science, Tianjin Medical University, Tianjin, China
[2]State Key Laboratory of Experimental Hematology, Tianjin Medical University, Tianjin, China
[3]The Province and Ministry Co-sponsored Collaborative Innovation Center for Medical Epigenetics, School of Basic Medical Science, Tianjin Medical University, Tianjin, China
[4]Department of Bioinformatics, School of Basic Medical Science, Tianjin Medical University, Tianjin, China
[5]Department of Hematology, Tianjin Medical University Tianjin General Hospital, Tianjin, China
[6]Department of Rheumatology and Immunology, Tianjin Medical University Tianjin General Hospital, Tianjin, China
[7]Department of Neurology and Institute of Neurology of First Affiliated Hospital, Institute of Neuroscience, and Fujian Key Laboratory of Molecular Neurology, Fujian Medical University, Fuzhou, China

[#]Co-first-authors;
[Δ]Co-second-authors;

[*]**Corresponding author:** Zhigang Cai, Professor, Ph.D.,
Mailing Address:
No.22 Qixiangtai Road,
Heping District, Tianjin 300070, China
E-Mail: us36zcai@tmu.edu.cn
Phone: (86)-022-18622633722

Running Title:

Neutrophil loss of Uba1 results in VEXAS-like symptoms

[Abstract word count: 200 words.]

[Main text word count: 11794 words.]

ABSTRACT

VEXAS (Vacuoles, E1 enzyme, X-linked, Autoinflammatory, Somatic) syndrome is a haemato-rheumatoid disease caused by somatic *UBA1* mutations in hematopoietic stem cells (HSCs). The pathogenic cell type(s) responsible for the syndrome are unknown and murine models recapitulating the disease are lacking. We report that loss of *Uba1* in various mouse hematopoietic cell types resulted in pleiotropic consequences and demonstrate that murine mutants with about 70% loss of Uba1 in neutrophils induced non-lethal VEXAS-like symptoms. Depletion of *Uba1* in HSCs induced extensive hematopoietic cell loss while depletion of *Uba1* in B or T cells, or in megakaryocytes induced corresponsive cell death but these mutants appeared normal. Depletion of *Uba1* in monocytes and neutrophils failed to induce cell death and the mutants were viable. Among the tested models, only depletion of *Uba1* in neutrophils induced autoinflammatory symptoms including increased counts and percentage of neutrophils, increased proinflammatory cytokines, occurrence of vacuoles in myeloid cells, splenomegaly and dermatitis. Residual Uba1 was about 30% in the mutant neutrophils, which disrupted cellular hemostasis. Finally, genetic loss of the myeloid pro-survival regulator *Morrbid* partially mitigated the VEXAS-like symptoms. The established VEXAS-like murine model will assist understanding and treatment of the newly identified autoinflammatory syndrome prevalent among aged men.

Key words:
VEXAS syndrome, Uba1, mouse models, autoinflammatory diseases, blood disorders, hematopoietic stem cells, neutrophils, *Morrbid,* IL-1β, clonal hematopoiesis

INTRODUCTION

It has been recognized for almost 40 years that protein ubiquitylation, or called as ubiquitination, describing a posttranslational process about transferring the 76-amino acid peptide "ubiquitin" on host proteins in nucleus or in cytoplasm, is critical for nearly all aspects of eukaryotic biology and cellular homeostasis (1). Aberrant protein ubiquitylation induces cellular dysfunction in many aspects of cell activities for neuronal cells or immune cells among other important cells, and may represent signs of diseases (2). Among multiple mechanisms of ubiquitin signaling, for example, ubiquitylation of histone in nucleus regulates genome stability and gene expression (3), and ubiquitin activation in the cytoplasm is the first step of the E1-E2-E3 enzymatic cascade, which are critical for almost of all of proteins inside the eukaryotic cells and maintains cellular homeostasis (4). Deficient protein ubiquitylation results in inadequate protein degradation, which in turn will generate overloaded proteins inside the cell and induce unfolded protein stress response (UPR) (5, 6).

In the E1-E2-E3 enzymatic cascade, the functions of enzymes E2 (~40 members) and E3 (> 600 members) have been broadly studied due to that they may regulate only a specific or a single aspect of physiology and loss of one of E2 and E3 members is insufficient to induce cell death (7, 8). However, due to the limited members of E1 (only 2 members in mouse and human, UBA1 and UBA6) and lethality induced by loss of one of UBA1 and UBA6, their function and action mechanisms in the *in vivo* model have not been well documented (9, 10). Interestingly, *UBA6* encodes a cytoplasm isoform only UBA6 while *UBA1* encodes two isoforms, UBA1a and UBA1b. UBA1a isoform is with nucleic signal and locates in the nuclei while UBA1b isoform is shorter in protein length and locates in the cytoplasm (11). Based on conditional knockout (CKO) models, role of *Uba6* in mouse has been implicated in neuronal cells (12). The regulation of polyalanine stretch by UBA6 is suggested in the critical biological process (13). However, the *in vivo* role of UBA1 in mammals, including the respective roles of UBA1a and UBA1b isoforms, remains largely unknown (14).

Although complete loss of *UBA1* or *UBA6* is hypothesized to induce cell death, somatic mutations in these two genes in clinical samples offer alternative approaches to understanding their functions in eukaryotic cells. It has been reported that a germ-line mutation in *UBA1* (i.e. p.Met539Ile or p.Ser547Gly) induces X-linked infantile spinal muscular atrophy, a dysfunction of nervous system (15, 16). Additionally, $UBA1^{M41L}$ mutation-induced loss of function of UBA1b isoform (p.Met41Leu) was implicated in a newly described autoinflammatory haemato-rheumatoid disease, the Vacuoles, E1 enzyme, X-linked, Autoinflammatory, Somatic (VEXAS) syndrome (17). The $UBA1^{M41L}$ mutation results in removal of the cytoplasm isoform UBA1b while the nucleic isoform UBA1a is unchanged. The VEXAS syndrome took place mostly in adult male patients while female patients were reported rarely, suggesting it is induced by loss-of-function of *UBA1* (18). About 200 following-up retrospective clinical studies describing about 500 patients with VEXAS syndrome further demonstrate that various mutations in *UBA1* are associated with this adult-onset severe disease affecting organs including blood, vascular, nose, ear, skin, lung and brain (18-33). In the first VEXAS report, loss of *UBA1b* homologs rather than *UBA1a* homologs in zebrafish by morpholino was described to induce systemic inflammation; however, the fish mutants were lethal and minimally reminiscent of the VEXAS symptoms in human (17). Recently, through cutting-edge gene editing strategy, a mouse cell line-based approach

(*in vitro* cell culture) and a human HSC-based approach (hosted by chimeric mice) for modeling VEXAS syndrome was reported by *Chiaramida et al* (34) and by *Molteni et al* in a meeting abstract (35). Although these two models are important and complementary for understanding pathology of VEXAS syndrome, a genetically reliable and easy-setup *in vivo* VEXAS-like animal model that could be maintained at the adult ages is still lacking.

To define the major responsible cell type(s) and recapitulate human VEXAS syndrome in mammals, in this study we aimed to generate murine models by genetically manipulating *Uba1* locus and to further explore the pathology and treatment of the autoinflammatory disease. We constructed various CKO models to dissect the discrete roles of *Uba1* in almost each major hematopoietic cell type including HSCs, lymphoid cells, megakaryocytes and myeloid cells. Our study demonstrates that loss of *Uba1* in neutrophils is critical for inducing VEXAS-like disorders and offer translational implications, suggesting that the VEXAS symptom in human is likely attributed to a combinational hematological and immunological consequence of *UBA1* point-mutation over a long-term journey of clonal hematopoiesis. Thus, complimentary to studies merely using clinical samples, our study suggests that mutant neutrophils are aberrant and equally as important as the mutant HSCs and play a critical role for driving the autoinflammatory disease. In addition, our study suggested that treatment with IL-1β/IL-1R1 inhibitors (Canakinumab or Anakinra) or genetic loss of the myeloid pro-survival regulator *Morrbid* partially mitigated the VEXAS-like autoinflammatory symptoms in the mutant mice.

RESULTS

A Cre/flox approach to model VEXAS syndrome

UBA1 in human and *Uba1* in mouse are at the X-chromosome. The encoded proteins (UBA1 vs. Uba1) shares the same protein length and almost the same protein molecular weight (1,058 amino acids; for the full-length isoform, 117.849 kDa in human vs. 117.808 kDa in mouse). The identity of the protein sequences is as high as 95% and similarity of that as high as 98% (**Figure S1A**). Although VEXAS syndrome is induced by a spontaneous somatic mutation in HSC *UBA1* in human (upper panel, **Figure 1A**), here we report results on Cre/flox-based CKO models, by observing the primary mutant mice or by transplantation of the mutant bone marrow (BM) cells in the chimeric mice. The outcomes suggest the CKO strategy is technically feasible and easy to model VEXAS syndrome. In addition, the VEXAS-like mutant mice could be maintained during adult age since we identified neutrophil loss of *Uba1* (null mutation) induces VEXAS-like symptoms (lower panel, **Figure 1A**). Due to unavailability of certain *Cre* strains, the present study has not covered the specific roles of *Uba1* for erythroid blasts, mast cells, eosinophils and basophils; but other major cell types in hematopoiesis system have been covered and described in detail. Here we report the results from the 9 different CKO mouse models covering deletion of *Uba1* in HSCs (3 lines in total), pan-lymphoid cells (2 lines in total; among them, 1 line for B cells and 1 line for T cells) and pan-myeloid cells (4 lines in total; among them, 1 line for megakaryocyte, 2 lines for monocytes/macrophages and 1 line for neutrophil).

As shown in the left panel of **Figure 1B**, we generated a flox strain at the *Uba1* locus where the Exon 6-8 will be removed when the $Uba1^{flox}$ mice were crossed with certain *Cre* lines. The flox strain appears normal as wild type mice (WT) in male and female (for male, $Uba1^{flox/y}$ is normal as $Uba1^{+/y}$; for female, $Uba1^{flox/flox}$ and $Uba1^{flox/+}$ are normal as $Uba1^{+/+}$). PCR genotyping with primers F1 and R1 successfully distinguished the flox allele from the WT allele (right panel, **Figure 1B**). As VEXAS syndrome is a disorder mostly affecting aged men, we mainly generated male CKO mutant mice (mutant male mice marked as *Cre;CKO* or $Cre;Uba1^{flox/y}$, and WT male mice as $Uba1^{flox/y}$) and collected related tissues for the following studies.

As CKO mice generally manifest chimerism of WT and mutant mRNA transcripts of *Uba1* in certain tissues, we first verified the disruption of the *Uba1* transcripts by aligning the bulk sequencing reads in the pool of all reads to the mouse reference genome. As shown in the **Figure 1C**, we observed that some sequencing reads indeed have no Exon 6-8, which is expected by the Cre/flox gene-targeting strategy (the CKO mice used for the mRNA transcript analysis are *S100a8Cre;CKO*; see also **Figure 5**). Removal of Uba1 Exon 6-8 by Cre results in 331-bp off and an early occurrence of a stop codon at the Exon 10 in the mRNA transcript. The putative truncated protein is predicted with 200 amino acids in protein length and as 22 kDa in protein molecular weight. Through the assays with the Uba1a-isoform-specific antibody, we failed to identify a real truncated protein, indicated by the arrow in **Figure 1D** and **E**, in the total BM cells or in the neutrophils of the *S100a8Cre;CKO*. Furthermore, in the total BM cells, we determined the average level of Uba1a isoform in the *S100a8Cre;CKO* mutant is 63% of that in WT controls (p=0.012, **Figure 1D**). In the purified neutrophils, we determined the average level of Uba1a isoform in the *S100a8Cre;CKO* mutant is 28% of that in WT controls, suggesting a dramatic depletion of Uba1a isoform in the

S100a8Cre;CKO mutant neutrophils (p=0.0001, **Figure 1E**). When using an alternative antibody sensitive to both Uba1a and Uba1b isoforms, we determined a similar level of Uba1a and Uba1b depletion (~31% of WT level, p=0.012, **Figure 1F**). Although this antibody is sensitive to both isoforms in mouse BM cells, expression of Uba1a isoform is detectable but is weaker than that of Uba1b isoform (**Figure 1F** and **G**). Interestingly, in the mouse and human cell lines, Uba1a and Uba1b isoforms appear to have similar expression level (**Figure 1G**).

We also conducted qRT-PCR assays and determined that residual levels of *Uba1* mRNA transcripts are about ~50% of WT level in the total BM cells and ~30% of WT level in purified neutrophils (**Figure S1B**). Although there is slight leakage of *S100aCre* in purified monocytes determined by qRT-PCR (fold change of mRNA: 0.78, p<0.001; **Figure S1B**), the protein level of residual Uba1 appear grossly normal in the monocytes from *S100a8Cre;CKO* mutants (fold change of protein: 0.87, p=0.1979; **Figure S1C**). Taken together, the results suggest that mouse Uba1 and human UBA1 are highly conserved and that our conditional disruption of the transcripts and protein isoforms by the Cre/flox approach is successful. Specifically, the residual levels of *Uba1* mRNA and Uba1 protein in the neutrophils of *S100a8Cre;CKO* mutant are about 30% of WT levels.

Conditional depletion of Uba1 in HSCs

As shown in **Figure 2A** and **B**, we tried three different HSCs-targeting *Cre* lines to dissect the role of *Uba1* in HSCs, which are atop the hematopoietic hierarchy, *Vav1Cre*, *Rosa26-Cre-Ert2* (labeled as R26CreErt2 here for simplicity*)* and *Mx1Cre*. *Vav1Cre* is active as early as embryonic day 9 (36). After several rounds of breeding, we failed to obtain any male *Vav1Cre;Uba1$^{flox/y}$* pups (**Figure 2A**, total male pups n=16, but *Vav1Cre;Uba1$^{flox/y}$* male pups n=0; chi-square test, p<0.05). We then turned to generate *R26CreErt2; Uba1$^{flox/y}$* or *Mx1Cre;Uba1$^{flox/y}$* by crossbreeding as they are alive when no drug induction is applied (tamoxifen for *R26CreErt2* and Poly I:C for *Mx1Cre*) (37, 38).

To dissect the role of *Uba1* in HSCs and following hematopoiesis, we constructed competitive bone marrow transplantation (cBMT) assays as shown in **Figure 2B**. BM cells from donor mice *Uba1$^{flox/y}$* were used as controls along with those from donor mice *R26CreErt2;Uba1$^{flox/y}$* or *Mx1Cre;Uba1$^{flox/y}$* as competitors. Of note, upon tamoxifen induction, *R26CreErt2* is expressed in all cell types (including HSCs); upon polyI:C induction, *Mx1Cre* is specifically activated in HSCs and used for dissecting roles of genes of interest in HSCs. As shown in **Figure 2C** to **G**, activation of the *R26CreErt2* by tamoxifen or activation of *Mx1Cre* by PolyI:C induced cell death in a large fraction of donor cells from *R26CreErt2;Uba1$^{flox/y}$* or *Mx1Cre;Uba1$^{flox/y}$* BM, suggesting that *Uba1* is indispensable for HSCs and following hematopoietic progenitor cells.

We were also interested in how long the primary *Mx1Cre;Uba1$^{flox/y}$* mice can survive after PolyI:C induction of *Uba1* depletion. As shown in **Figure 2H**, after administration of PolyI:C, the animals cannot survive longer than 3 weeks (n=5 mice per group, p<0.001). As *Mx1Cre* is also active in multipotent progenitor cells (MPP, developmentally close to megakaryocyte-erythroid progenitor, MEP) and the half-life of red blood cells is very short (~24 hours), one of the direct reasons for the death of

Mx1Cre;Uba1$^{flox/y}$ mutants is the shortness of red cell supply. In conclusion, these results demonstrated that depletion of *Uba1* at the HSC level induces a quick and extensive death in almost all kinds of hematopoietic cells.

Conditional depletion of Uba1 in lymphoid cells or megakaryocytes

We then tested depletion of *Uba1* at the mature blood cells in the hematopoietic and immune system. Two *Cre* lines for lymphoid cells (*Cd4Cre* and *Cd19Cre*) (39, 40), and one *Cre* line for megakaryocytes (*Pf4Cre*) were used (41). As shown in **Figure 3A** to **D**, dramatically decreased amount of $Cd4^+$T cells or $Cd19^+$B cells were readily observed in *Cd4Cre;Uba1$^{flox/y}$* or *Cd19Cre;Uba1$^{flox/y}$* mice (cell-depletion efficiency: 50%~70%). However, the mutant animals appear normal and survive over than 12 months in the specific-pathogen-free (SPF) facility. As shown in **Figure 3E** and **F**, ~50% depletion of megakaryocytes and platelets were also observed in *Pf4Cre;Uba1$^{flox/y}$* but the mutant animals also appear normal and no VEXAS-like symptoms were observed over the age of 12-month old. These results demonstrate that conditional depletion of *Uba1* in lymphoid cells or megakaryocytes successfully resulted in corresponsive cell death but failed to induce VEXAS-like abnormalities in mice.

Conditional depletion of Uba1 in monocytes by Lyz2Cre or Cx3cr1Cre

We also tested depletion of *Uba1* in monocytes and macrophages. For this aim, two *Cre* lines for monocytes and macrophages were used in the study: *Lyz2Cre* and *Cx3cr1Cre* line (42, 43). As shown in **Figure 4A** to **D**, no significant reduction of myeloid cells was observed in *Lyz2Cre;Uba1$^{flox/y}$* or *Cx3cr1Cre;Uba1$^{flox/y}$*. Although we occasionally observed vacuoles in few myeloid cells from the blood cells of *Lyz2Cre;Uba1$^{flox/y}$*, both *Lyz2Cre;Uba1$^{flox/y}$* and *Cx3cr1Cre;Uba1$^{flox/y}$* mice appear quite normal. To confirm the *Cre* activity induced by *Lyz2Cre*, we crossed *Lyz2Cre;Uba1$^{flox/y}$* with *tomato-lox-GFP* line (labeled as *lox-GFP* here for simplicity) (44). The mice *Lyz2Cre;lox-GFP* and *Lyz2Cre;lox-GFP;Uba1$^{flox/y}$* were generated respectively. Expression of GFP in *Lyz2Cre;lox-GFP* and *Lyz2Cre;lox-GFP;Uba1$^{flox/y}$* indicates the activity of *Lyz2Cre* and the depletion of *Uba1* in the *Lyz2Cre;lox-GFP;Uba1$^{flox/y}$* compound mutants. As shown in **Figure S1D** and **E**, surprisingly loss of *Uba1* even resulted in a higher portion of myeloid cells in the peripheral blood.

To further characterize the myeloid cell-depletion of *Uba1* by *Lyz2Cre*, we performed the qRT-PCR and immunological blotting assays. As shown in **Figure 4E** and **F**, a significant reduction of Uba1 is detected in the monocytes of *Lyz2Cre;Uba1$^{flox/y}$* (Uba1 residual expression is about 24% of control level, $p<0.001$). A slight reduction of Uba1 is also detected in neutrophils of *Lyz2Cre;Uba1$^{flox/y}$* compared to the controls (residual level is about 75% by qRT-PCR, $p<0.001$ and about 79% by western blotting, $p=0.116$; **Figure 4E** and **F**), suggesting slight leakiness by *Lyz2Cre* in neutrophils in the *Lyz2Cre; Uba1$^{flox/y}$* mutants. Taken together, these results demonstrated that monocyte-based depletion of *Uba1* failed to induce VEXAS-like abnormalities in mice, and intriguingly somehow mature myeloid cells with loss of *Uba1* appear to have extended life-span rather than to be vulnerable to cell death.

Conditional depletion of Uba1 in neutrophils induces VEXAS-like phenotypes

As shown above, although the *Lyz2Cre* strain in the study demonstrated slight leakiness

in neutrophils, it is not a strong and reliable *Cre* strain for targeting genes in neutrophils (left panel of **Figure 4E**; upper panel of **Figure 4F**). However, the fraction of neutrophils in BM (about 50%) is almost 5 to 10-fold of that of monocytes (about 5%~10%). We then tried depletion of *Uba1* in neutrophils using the *S100a8Cre* line, which is widely used for knocking-out genes of interest in neutrophils (45). Most of the *S100a8Cre;Uba1*$^{flox/y}$ mutant mice appear normal at the age 2~3-month-old while a few of *S100a8Cre;Uba1*$^{flox/y}$ mice appear abnormal as early as 1-month old (frequency: 10.6%, 5 out of 47). When the *S100a8Cre;CKO* mice grew up (about 4-month-old), we started to observe their kink tails (**Figure 5A**) and flare nose (**Figure 5B**). And such aberrations turned to be more obvious at older ages (i.e. during 6~12-month-old). Additionally, hair loss on their back started to be observed (**Figure 5A**), a sign of dermatitis. Furthermore, after examining the entire body, we also observed swollen toes and pigmentation on the knuckles of paws (including the front and the rear paws) in the *S100a8Cre;CKO* mutant mice (**Figure 5C**). We don't know the exact mechanism(s) by which the pigmentation appears on the knuckles of the paws.

When we expanded the production of *S100a8Cre;Uba1*$^{flox/y}$ male mutant mice by active breeding, we were also able to obtain female mutants (*S100a8Cre;Uba1*$^{flox/flox}$) in the offspring. The female mutant mice manifest identical body appearances described above in the male mutant mice but all types of the controls are as normal as WT, including the *S100a8Cre* strain itself (male and female), *Uba1*$^{flox/y}$ male, *Uba1*$^{flox/+}$ and *Uba1*$^{flox/flox}$ female, and *S100a8Cre;Uba1*$^{flox/+}$ female. In addition, we alternatively husbanded the mutant mice (*S100a8Cre;Uba1*$^{flox/y}$ or *S100a8Cre;Uba1*$^{flox/flox}$) in a clean-grade air condition for 12 months. The mutant mice in the clean-grade facility showed similar body symptoms as that in the SPF facility but no obvious pneumonia or colitis were observed (n=5). Taken together, these phenotypic observations confirmed that the appearances of kink tails, flare noses, and knuckle pigmentations on paws were induced by *S100a8Cre*-mediated depletion of *Uba1* in the mutant male and female mice and that husbandry of the mutant mice in the SPF-grade or clean-grade facility manifest similar body appearances as described in **Figure 5A-C**.

To examine any aberrant hematological parameters in the mutant mice with similarities to VEXAS syndrome in human, we quantified the blood cells by hematological analyzers and flow cytometry. As shown in **Figure 5D**, the *S100a8Cre;CKO* mice manifest increased white blood cell (WBC) counts (fold change: 1.5, $p<0.05$), increased neutrophil (NE) counts (fold change: 1.9, $p<0.01$) and increased neutrophil percentage in WBC (NE%; fold change: 1.2, $p<0.05$), which are hallmarks and indications of autoinflammatory diseases including VEXAS syndrome. Furthermore, a slight but significant increase of mean corpuscular volume (MCV) was also determined in *S100a8Cre;CKO* mutants (fold change: 1.05, $p<0.05$) (**Figure 5D**). Of note, MCV is recognized as one of the key laboratory tests for VEXAS syndrome and increase of MCV indicates anemia in clinic (17). As shown in **Figure S2A-B**, a slightly impaired erythropoiesis in the BM was observed in the *S100a8Cre;CKO* mutants. The differences in red blood cell (RBC) counts between *S100a8Cre;CKO* mutants and the WT controls did not reach the bar of statistical significance. We also conducted flow cytometry to measure the changes in compartments of mature blood cells the *S100a8Cre;CKO* mutant mice or hematopoietic progenitor cells in BM. As shown in **Figure 5E-F**, fraction of neutrophils ($Gr1^+CD11b^+$) in PB is increased while that of B cells ($CD19^+$) is decreased, consistent to results from hematological analyzer (**Figure 5D**).

We also examined the existence of vacuoles in the myeloid cells of the *S100a8Cre;CKO* mutants, one of the hallmarks of VEXAS syndrome (17). As shown in **Figure 5G**, we observed about 10% of myeloid cells (mainly are neutrophils) are with vacuolar characteristics. As shown in **Figure S2C-D**, we also observed rare occurrences of vacuolization in the myeloid progenitor cells and erythroid cells of BM from the *S100a8Cre;CKO* mutants. Compared to WT controls, fraction of HSCs in the mutants is comparable while that of granulocyte-macrophage-progenitor (GMP) and $Lin^{-}Sca1^{-}cKit^{+}$ cells (LSK) appears to be elevated (**Figure S3A** and **B**), suggesting inflammation regulation of hematopoiesis in BM. Furthermore, H&E staining of skin, tail and paws indicate dermatitis and infiltration of inflammatory immune cells in the paws (**Figure S4A-C**). However, we did not observe obvious chondritis in the nose in the *S100a8Cre;CKO* mice (relapsing polychondritis [RP] in nose and ear is another one of hallmarks of VEXAS syndrome in human) (17). H&E staining of lung tissue identified minimal alteration of immune cells and the stromal cells but single-cell RNA-sequencing analysis revealed increased inflammatory scores in the immune cells (**Figure S4** and **S5**). Single-cell RNA-sequencing analysis of skin tissue, however, failed to identify obvious alterations, probably due to insufficient capture of immune cells in the mutant skin tissues by our technical platforms or approaches (**Figure S6**). In summary of the phenotypes, *S100a8Cre;CKO* mice have VEXAS-like symptoms, including inflammatory hematological parameters, vacuoles in neutrophils (~10%), dermatitis, swollen paws. In addition, a frequent pigmentation on knuckles of mutant paws, which was not reported in fingers or toes of patients with VEXAS syndrome. Finally, the mutant mice did not show visible RP in their ears, which were frequently reported in patients with VEXAS syndrome.

We then measured the serological parameters in the mutant mice as proinflammatory cytokine level is a key for several autoinflammatory diseases including VEXAS syndrome (17). A 10-cytokine panel was used for quantifying proinflammatory and anti-inflammatory cytokines. Among them, three proinflammatory cytokines IL-1β, IL-6 and TNFα all are significantly upregulated in the serum with fold change between 2 and 40 accordingly (**Figure 5H**, n=9 mice for WT group and mutant group**;** see **Figure S7A** for the full plots of the 10 cytokines in the tested mutant animals). Interestingly we observed positive correlation between the three proinflammatory cytokines (IL-1β, IL-6 and TNFα) but IFNγ appear unchanged (**Figure S7B**), suggesting the expression of the three classical proinflammatory cytokines are systematically coordinated in the VEXAS-like mice. According to the examinations on mouse body appearance, analysis of blood cells, and serum expression of cytokines, these results demonstrate that the *S100a8Cre;CKO* mutant mice manifest VEXAS-like autoinflammatory haemato-rheumatoid disorders.

Ubiquitination and cell survival advantage for the mutant neutrophils

We also confirmed grossly normal expression of Uba6 in total BM cells or in purified neutrophils of *S100a8Cre;CKO* mice (**Figure 6A**). In addition, we demonstrated significantly down-regulated poly-ubiquitylation (poly-Ub) level and up-regulated free-ubiquitin (free-Ub) in the mutant neutrophils from the *S100a8Cre;CKO* mice (**Figure 6B**).

Furthermore, the increased count of neutrophils in the *S100a8Cre;CKO* mutants is

intriguing as this abnormality is in line with what we observed in the *Lyz2Cre;Uba1*$^{flox/y}$ mice. Profiling the hematopoiesis by flow cytometry suggested a biased myelopoiesis (myeloid-skewing) in the *S100a8Cre;CKO* mice (**Figure S3A-B**). In addition, the body weight of the *S100a8Cre;CKO* mutant mice is less than that of WT controls while the weight of spleen is greater than that of WT controls, suggesting a splenomegaly (a sign of leukemia or inflammation) in the mutant mice (**Figure S3C**).

Although in neutrophil we observed a slightly increased apoptosis activity determined by Annexin-V-marked flow cytometry (**Figure S3D**), we functionally demonstrated an overall survival advantage of *S100a8Cre;CKO* myeloid cells, specifically for neutrophils, by three independent *in vivo* approaches. The first approach is similar to what we have shown in *LyzCre;lox-GFP* (**Figure S1D** and **E)**: using the GFP reporter line along with flow cytometry analysis. The GFP reporter experiments suggest that a comparable or even higher fraction of $Gr1^+$ cells or GFP^+ cells in the *S100a8CreCKO;lox-GFP* compared to that in the *S100a8Cre;lox-GFP* control (**Figure S3E** and **F**). The second approach is through cBMT assays (see **Figure 6C** for the experiment scheme). As shown in **Figure 6D**, the donors from *S100a8Cre;CKO* manifest a phenotype of clonal hematopoiesis, which was also indicated in the human VEXAS syndrome (46). The cBMT assays suggest that the *S100a8Cre;CKO* neutrophils have a survival advantage. The third approach is to directly measure the half-life of neutrophils by BrdU staining and tracing (47). Compared to the WT neutrophils, the *S100a8Cre;CKO* neutrophils manifest significantly extended half-life (fold change: 1.35, p=0.03; $t_{1/2}$ of mutant neutrophils = 45.3±0.98 hrs vs. $t_{1/2}$ of WT neutrophils = 33.52±4.85 hrs; n=3~4 assay repeats per group and 6 animals were recruited for a BrdU-chasing assay; **Figure 6E** and see **Methods**). Taken together, using three independent *in vivo* experimental assays, we demonstrated that the mutant neutrophils lacking expression of *Uba1* in the *S100a8Cre;CKO* somehow have growth or survival advantage against the WT controls in the BM.

Disturbed neutrophil homeostasis revealed by assays on ROS, proinflammatory cytokines and phagocytosis

As *S100a8Cre* is mainly active in neutrophils, we wondered if any cell-autonomous abnormalities exist in *S100a8Cre;CKO* neutrophils with regards to reactive oxygen species (ROS) production, proinflammatory cytokine expression (i.e. IL-1β, IL-6 and TNFα), inflammasome activation (i.e. NLRP3), neutrophil extracellular traps (NETs) formation and phagocytosis capability on bacteria. As shown in **Figure 7A**, by flow cytometry we determined that the mutant animals had increased fraction of ROS^{high} neutrophils in the BM and increased expression of ROS in neutrophils. As shown in **Figure 7B**, by western blotting we determined the mutant neutrophils manifested significant increased expression of myeloperoxidase (MPO), IL-6, TNFα and Nlrp3 (fold change is between 1.6 to 7.3; $p \leq 0.05$). Expression of Caspase-1 appeared to be increased (fold change is about 1.5; $p = 0.13$). We also performed enzyme-linked immunosorbent assay (ELISA) to determine the cell autonomous expression of proinflammatory cytokines IL-6, IL-1β and TNFα in the neutrophils. As shown in **Figure 7C,** both the secretion levels and intracellular levels of these three proinflammatory cytokines are significantly increased in the mutant neutrophils, consistent with the serum results shown in the **Figure 5H**.

Aberrant activities of NETs and phagocytosis is suggested in myeloid cells from patients with VEXAS syndrome (17). By staining with NETs markers MPO and CitH3, we determined that the *S100a8Cre;CKO* neutrophils had increased count of NETs in the *ex vivo* assays (**Figure 8A**). We experimentally examined the phagocytosis capability of the mutant neutrophils by co-culture of neutrophils and GFP-labeled *E. coli* bacteria (see **Figure 8B** for the experimental scheme). As shown in **Figure 8C**, the mutant neutrophils appeared to have greater phagocytosis capabilities (n = 3 biological repeats, $p<0.01$).

Verification of neutrophil-specific loss of Uba1 by single-cell transcriptomic analysis

As shown in **Figure 1D-F**, we experimentally determined neutrophil depletion of Uba1 at both the mRNA and protein isoform level (residual level: ~30%, indicating 70% depletion efficiency). To unbiasedly and orthogonally verify the exact cell type(s) with loss of *Uba1* expression in *S100a8Cre;CKO*, we took advantage of single-cell RNA-sequencing (scRNA-seq) technologies. As shown in **Figure 9A**, a total of 11,204 and 10,054 BM cells were included in the UMAP plot composing cells from 3 donors of *Uba1*$^{flox/y}$ mice and 3 donors of *S100a8Cre;CKO* mice. The major BM cell types were annotated (11 cell types in total, left panel of **Figure 9A**). The fractions of HSPCs (mainly are GMPs) and neutrophils are marked by expression of *Ms4a3* and *Cebpd* respectively (right panel of **Figure 9A**). A large reduction of *Uba1* transcripts in Pro_Neutrophils and Neutrophils are detected (residual level: 27% and 29% respectively, indicating ~70% depletion efficiency in both; **Figure 9B**) along with subtle reduction of *Uba1* in monocytes (residual level: 83%, indicating ~20% depletion efficiency; **Figure 9B**). We did not detect dramatic reduction of *Uba1* in other cell types including HSPCs (**Figure 9B**). These results provide orthogonal evidence suggesting a marked depletion of *Uba1* in neutrophils (pro-neutrophil and mature neutrophil) but not in other hematopoietic cell types (i.e. HSPCs and monocytes) in the *S100a8Cre*-induced CKO.

Disturbed neutrophil homeostasis revealed by the scRNA-seq analysis

To further comparing the BM activity in *Uba1*$^{flox/y}$ and *S100a8Cre;CKO* mice, we also took advantage of the scRNA-seq datasets to measure the cell homeostasis by scoring activity of various functional aspects in the neutrophils using the module-score computational function in the Seurat toolkits (see **Methods** for details). The cells (Pro_Neutrophils and Neutrophils) used for the scoring analysis are highlighted in **Figure 10A**. As shown in **Figure 10B**, the ubiquitylation scores were readily decreased in Pro_Neutrophils and Neutrophils of the mutants, consistent to the loss-of-function of Uba1 in the cells. Scoring the activity of UPR, inflammation, apoptosis, necroptosis, ROS, and NETs formation further suggested disturbed cellular homeostasis (**Figure 10C-F** and **Figure S8A-D**). As shown in **Figure 10G**, volcano plots highlight significant downregulation of *Uba1* and significant upregulation of inflammation-related genes *Ifit1* and *Ifit3*. We also validated the results of scRNA-seq analysis using the bulk RNA-seq datasets on BM cells. As shown in **Figure S8E-F**, we detected upregulation of inflammatory genes *Il1r1* and other genes in the inflammatory pathways.

In addition to the transcriptomic analysis, as shown in **Figure S9A-H**, LC/MS-based proteomic analysis of the BM cells from *Uba1*$^{flox/y}$ donors and *S100a8Cre;Uba1*$^{flox/y}$

donors (n=3 respectively) also demonstrate depletion of Uba1 in the BM (residual level is about 57.1%) and disturbed immune responses including complementary response, inflammatory response and NETs formation. Taken together, results from single-cell RNA-seq datasets, bulk RNA-seq datasets, and protein LC/MS datasets all indicated that depletion of *Uba1* in the *S100a8Cre;CKO* mutants resulted in various aspects of disturbed cellular or immunological activities including increased UPR, ROS activity and NETs formation. These immune-related abnormalities were also described in BM cells from patients with VEXAS syndrome (17).

Inhibition of IL-1β/IL-1R1 signaling partially mitigated the VEXAS-like symptoms

It is well known that autoinflammatory diseases are generally modulated by IL-1 signaling (48). We tried treatment for the *S100a8Cre;CKO* mutants with Anakinra (a peptide-like antagonist for IL-1R1) or Canakinumab (a monoclonal antibody for IL-1β). As shown in **Figure 11A-B** and **Figure S10A-C**, the present treatment regime with Anakinra or Canakinumab only partially mitigated the symptoms in *S100a8Cre;CKO*: WBC counts were decreased but neutrophil counts appeared unchanged.

Genetic loss of Morrbid ameliorated the VEXAS-like symptoms

In our previous anti-leukemia studies, we demonstrated that the human-mouse conserved lncRNA *Morrbid* is a pro-survival regulator for myeloid cells and has a role in myeloid-lineage leukemogenesis (49-52). In addition, elevated expression of *Morrbid* is readily detected in the transcriptomic dataset of BM cells in the *S100a8CreCKO* mutants (**Figure S10D**). According to the rationale shown in **Figure 12A**, we assessed the role of *Morrbid* by generating the compound mutant *S100a8CreCKO;Morrbid*$^{+/-}$ (*Morrbid*$^{+/-}$ heterozygous mice manifest similar short life-span of myeloid cells as *Morrbid*$^{-/-}$ homozygous mice). As shown in **Figure 12B-D**, genetic loss of *Morrbid* also partially mitigated the VEXAS-like symptoms including decreased counts of WBC and MCV, disappearance of pigmentation in the paw knuckles and decreased serum levels of proinflammatory cytokines.

DISCUSSION

As illustrated in **Figure 13**, we align the findings from the clinical studies of VEXAS syndrome in human (**Figure 13A-B**) and the results from our study in mice (**Figure 13C-D**). In the **Supp. Material Table-S1**, **Table-S2**, **Table-S3** and **Table-S4**, we also provide four angles covering the comparison of various aspects of human VEXAS syndrome and our mouse modeling in details. Overall, it is persuasive that VEXAS syndrome in human is induced by the comprehensive and synthetic consequence of somatic, pathogenic and loss-of-function of *UBA1* mutations in HSCs; however, the nine CKO murine models in the present study recapitulate consequences of *Uba1* loss (null mutation) in certain hematopoietic cell types. Thus the big difference in appearance of VEXAS in human and phenotypes in various *CKO* or chimeric mice e could be summarized as "a holistic and synthetic effect" in human vs. "a limited and cell-type specific effect" in mouse presented here.

Interestingly it was suggested by some clinical studies that mutant monocytes with somatic point mutations in *UBA1* may contribute VEXAS autoinflammatory symptoms in human (17, 53, 54). However, our study does not support the arguments that mutant monocytes alone with a null mutation of *Uba1* intrinsically play a role in VEXAS-like syndrome in mice. Among the nine *Uba1*-CKO mutants described here, only *S100a8Cre;CKO* mice induces VEXAS-like symptoms. In addition to induce gene knock-out in mature monocytes and macrophage*, Lyz2Cre* is reported to have leakage in neutrophils to certain extent. As *Lyz2Cre;CKO* mice don't show phenotype as strong as *S100a8Cre;CKO*, Cre activity in neutrophil for *Lyz2Cre* is probably not as strong as that for *S100a8Cre*. An alternative explanation is that the timing of *S100a8Cre* is probably earlier than that of *Lyz2Cre* for neutrophil depletion of Uba1. Using qRT-PCR and immunological blotting, we experimentally verified that *Lyz2Cre* does have slight leakage in neutrophil but the residual Uba1 protein maintained as high as ~78%, while residual of Uba1 protein in monocytes is about 24% (**Figure 4E** and **F**). Lack of abnormalities in *Cx3cr1Cre;CKO* mice provide further evidence supporting that monocyte or macrophage-loss of *Uba1* is not sufficient to induce VEXAS-like phenotypes in murine models. In addition, fraction of monocytes and macrophages in the BM and PB is much less than that of neutrophils, which may represent another reason for lacking of VEXAS-like phenotype in *Lyz2Cre;CKO* and *Cx3cr1Cre;CKO*. Through measuring the gene expression and cell activity by scRNA-seq, we again validated the neutrophil-specific loss of *Uba1* in *S100a8Cre;CKO* and disturbed cellular and immunological activities in various aspects (ubiquitylation, UPR, inflammation, ROS and NETs), which are related to the intrinsic function of Uba1 and neutrophils (**Figure 9** and **10**).

We are aware that *S100a8Cre;CKO* mice (neutrophil only-based $Uba1^{null}$) are indeed not as the same as the point mutations in human (chimeric but all types of hematopoietic cells-based $UBA1^{mut}$). However, both mutations are loss-of-function, which is one of the key genetic etiologies of VEXAS syndrome. Another one of key genetic etiologies is the threshold of variant allele value of the $UBA1^{mut}$, which is worthwhile to be asked in future as well in clinic. Reversing such loss-of-function defects could guide future development of interventions for this important biological process mediated by UBA1. When disrupting the function of Uba1 in almost of each major cell type in the bone marrow, our study demonstrates that null-mutations of *Uba1* in neutrophils rather than in other tested hematopoietic cells are critical for inducing VEXAS-like symptoms.

Nonetheless, installing a point-mutation in mouse HSCs by gene editing is undoubtedly necessary to fully recapitulate VEXAS symptoms in mice, which is suggested in a recent meeting abstract and in a mouse myeloid cell line (34, 35).

Human UBA1 and mouse Uba1 are highly conserved and critical for eukaryotic cells. A quick and extensive death of hematopoietic cells took place in the HSC-wise depletion of *Uba1* (*Vav1Cre*, *R26CreErt2* and *Mx1Cre*-mediated respectively) suggesting HSCs with a null mutation of Uba1 (HSC-$Uba1^{null}$) are not tolerated at all. In the context of our HSC-targeting $Uba1^{null}$ studies, tolerance of somatic mutations in human HSC (i.e. $UBA1^{M41L}$) is quite intriguing and suggests further functional studies are required to ask if compensation function of UBA1a isoform or other compensation mechanisms (i.e. UBA6) exist in human HSC with $UBA1^{M41L}$. Of note, such two types of compensation mechanisms unlikely take place in mouse with $Uba1^{null}$ since Uba1a isoform is also depleted and Uba6 expression appear normal (**Figure 1D-E** and **Figure 6A**). Importantly, no VEXAS-like phenotypes were observed in the two HSCs-targeting chimeric mice with various chimeric fractions as analyzed in cBMT assays using *Mx1Cre;*CKO or *R26CreErt2;*CKO donor cells. These results further suggest that HSC-based $UBA1^{M41L}$ is unequal to HSC-based $UBA1^{null}$. "*Tolerated or not tolerated*" and "*pathogenic or not pathogenic*", represent two key questions in future to ask each individual *UBA1* variant among the full spectrum of mutations identified in the available VEXAS syndrome cohorts (16, 18, 23, 26, 28).

Although we provided data with regards to the intolerance of megakaryocytes by *Pf4Cre*-CKO, the cell-type-dependent tolerance and pathogenicity of erythroid blast and megakaryoblast, among other intermediate myeloid and lymphoid progenitors and blast cells, will still be one of the interesting questions to ask in future (i.e. experimental and functional examination). For this goal, using VEXAS-conditioned hematopoietic cells for a direct test under the *ex vivo* or *in vitro* experimental settings are also necessary. In addition, inducible *Cre* lines targeting hematopoietic progenitors (i.e. GMP, MEP and lymphoid progenitor) rather than HSCs will be worthwhile too to dissect the cell-type specific role of Uba1 along the full trajectory and each branch and hierarchy level of hematopoiesis.

In contrast to intolerance of $Uba1^{null}$ for HSCs, we uniformly observed the tolerance of $Uba1^{null}$ for monocytes and neutrophils, which were also observed in human mutant monocytes and neutrophils with $UBA1^{M41L}$ (17). Although flow cytometry-based apoptosis profile of mutant neutrophils suggests a higher apoptotic activity, we provided couples of alternative *in vivo* evidences supporting the survival advantage of mutant neutrophils when comparing with the normal neutrophils: (a) hematological cell counts in the peripheral blood, (b) cBMT assays, (c) half-life tracing by BrdU staining, and (d) lox-GFP-based genetic tracing. We speculate that the increased expression of pro-inflammatory cytokines IL-6, IL-1β and TNFα is the driver of the survival advantage of the mutant neutrophils and a positive feedback loop appears to take place in the VEXAS disease progression. Such a positive-feedback loop model has been proposed in our previous studies for explaining *TET2* mutations and clonal hematopoiesis and downstream regulators including IL-1β, IL-6, *Morrbid* and *Ptx3* are important for the *TET2* mutation-mediated hematopoietic and immunological abnormalities (49-51, 55). Of note, "clonal hematopoiesis" observed by the cBMT assay in the study is simply attributed to neutrophil loss of *Uba1* in the donor cells. It would be interesting to test in clinic in future if mitigating clonal hematopoiesis and

such positive-feedback loop brings any benefits for VEXAS syndrome patients (29, 46, 55).

Since VEXAS syndrome in human is a synthetic and holistic effect of all aspects of mutant hematopoietic cells carrying somatic *UBA1* mutations, it therefore will be required in future to generate compound *Cre* lines to test if stronger phenotype take place (i.e. generating *Lyz2Cre;S100a8Cre;Uba1*$^{flox/y}$). Furthermore, Anakinra, an inhibitor of IL-1/IL-1R1 signaling, and Ruxolitinib, an inhibitor of JAK2 signaling, have been reported to treat VEXAS syndrome (56, 57). It will be interesting to test if combination of these two drugs alleviate the autoinflammatory symptom in *S100a8Cre;CKO* mice. In addition, in our recent work on *Pstpip2*-KO induced autoinflammatory disease chronic multifocal osteomyelitis and in *Ncf2*-KO induced chronic granulomatous disease, we demonstrated that genetic loss of *Morrbid* mitigated these two autoinflammatory diseases too (58, 59). In addition to its function in anti-leukemia, targeting *Morrbid* (i.e. anti-*Morrbid* by antisense oligos) may represent a valuable strategy for inhibiting autoinflammation in clinical management. In future, additional pre-clinical studies that are comprehensively targeting IL-6, IL-1β and TNFα are necessary to assess the efficacy of anti-inflammation treatment for VEXAS.

Limitation of the study

In the present study we introduced a null version of mutation in *Uba1* rather than a point mutation like *Uba1*^{M41L} in murine models. Furthermore, multiple *Uba1*$^{non\text{-}M41}$ variants were reported. However, it should be cautious that the pathogenicity of those *non-M41* variants require functional experiments to validate (16, 18, 23, 26, 28). Our animal model studies provide an indirect but complementary and timely understanding of VEXAS syndrome. In addition, the present study has not covered the respective roles of *Uba1* for erythroid blast, mast cells, eosinophils and basophils. To fully dissect the role of *Uba1* in hematopoietic system, additional *Cre* lines are required to breed with the *Uba1* flox strain. Furthermore, our preliminary phagocytosis experiments indicated that the mutant neutrophils appear to have stronger NETs and phagocytosis capabilities. Given that the easy maintenance of the *S100a8Cre;Uba1*$^{flox/y}$ colonies, it will be interesting to test the mutant mice manifest any aberrations in additional inflammatory or traumatic challenges including pathogen-host immunity, trauma, and cancer immunity (50, 58, 60).

Conclusion

In conclusion, we report a VEXAS-like mouse model *S100a8Cre;Uba1*$^{flox/y}$ for mimicking an autoinflammatory disease recently identified in human, the VEXAS syndrome. Using the other eight CKO models, we also demonstrate that targeting certain hematopoietic cell types, rather than neutrophils, failed to manifest VEXAS-like symptoms. These results well document the intrinsic and diversified functions of Uba1 in mammal hematopoiesis and immunity-related cells and suggest cell-type-dependent pathogenicity of *UBA1*^{mut} in human VEXAS syndrome. The VEXAS-like mouse model *S100a8Cre;Uba1*$^{flox/y}$ will assist further understanding of VEXAS syndrome and warrant future development of effective treatments for the autoinflammatory disease highly prevalent among aged men.

Footnote

When our study was under revision, *Molteni et al* published their meeting abstract as a peer-reviewed report (61). Interestingly their experimental assays on gene-edited HSCs suggest that in the cell culture erythroid cells are not tolerated to the $UBA1^{M41L}$ point mutation.

METHODS

See **Supplemental Material** for Methods in details about mice strains and experimental procedures.

Statement regarding sex as a biological variable. As VEXAS syndrome is a disorder mostly affecting aged men, we mainly generated male CKO mutant mice (*Cre; Uba1$^{flox/y}$*) and collected the tissue samples from the male mutant mice for the assays described in the study. As we stated in the Results, for *S100a8Cre* mediated CKO models, the male mutant *S100a8Cre;Uba1$^{flox/y}$* and the female mutant *S100a8Cre;Uba1$^{flox/flox}$* manifest identical aberrances of body appearances but we still mainly used *S100a8Cre;Uba1$^{flox/y}$* for all described analysis and used *Uba1$^{flox/y}$* as WT controls.

Study approval. The animal study was approved by Tianjin Medical University Laboratory Animal Resource Center and experiments were conducted according to the protocol.

Data availability. The "Supporting data values" file for the Figures is provided in the **Supplemental materials**.
Raw bulk RNA-seq and scRNA-seq data in this study has been deposited in China National Center for Bioinformation/Beijing Institute of Genomics: https://ngdc.cncb.ac.cn/bioproject/browse/PRJCA025038 (GSA: CRA015841).
Proteomic data and scRNA-seq Matrix and have been deposited in https://ngdc.cncb.ac.cn/omix/release/OMIX006177 (OMIX006177) and https://ngdc.cncb.ac.cn/omix/release/OMIX006178 (OMIX006178).

Statistical analysis. Statistical analysis was performed using GraphPad Prism 9. If not stated else, data in figures are presented as mean ± SEM. One-way ANOVA with an uncorrected Fisher's test or 2-tailed Student's *t*-test was used to determine significant differences between groups. A *p* value of less than 0.05 was considered statistically significant.

Author contributions

ZC is the guarantor of the study. ZC conceived, designed, supervised the study, analyzed the data and wrote the manuscript. GD generated mouse models, monitored phenotypes, validated the neutrophil or monocyte depletion of Uba1 and phagocytosis assays, validated normal expression of Uba6; JL generated mouse models, monitored phenotypes, validated the neutrophil or monocyte depletion of Uba1, levels of Poly-Ubiquitin and free-Ubiquitin, levels of cytokines, ROS and inflammation pathways; WJ, HZ, YW, and ZW generated mouse models, monitored phenotypes, performed scRNA-seq and proteomic analysis, assisted the protein and RNA experiments, analyzed data. KX, JZ, LM, YM, LCC, QZ, HW, WW, and YF assisted the experiments and maintenance of mouse models. All authors edited and approved the manuscript.

Acknowledgements

We thank our colleagues for technical support, critically reading our manuscript, and their suggestions to improve the manuscript. We would also like to thank Drs. Liu, Li, Ding, Zhang and Yu (Tianjin Medical University School of Basic Medical Science), and Cheng (State Key Laboratory of Experimental Hematology) for sharing mice.

Funding

This work was supported in part by grants from the Tianjin Medical University Talent Program (to ZC), grants from State Key Laboratory of Experimental Hematology (to ZC), grants from Tianjin Key Laboratory of Inflammatory Biology (to ZC), and by grants from National Natural Science Foundation of China (NSFC) (to ZC, No. 82371789, No.82170173).

Disclosures of Competing Interests

ZC is a scientific advisor to Beijing SeekGene BioSciences Co. Ltd. The other authors declare no potential conflict of interest.

REFERENCES

1. Damgaard RB. The ubiquitin system: from cell signalling to disease biology and new therapeutic opportunities. *Cell Death & Differentiation.* 2021;28(2):423-6.
2. Beck DB, Werner A, Kastner DL, and Aksentijevich I. Disorders of ubiquitylation: unchained inflammation. *Nature Reviews Rheumatology.* 2022;18(8):435-47.
3. Mattiroli F, and Penengo L. Histone Ubiquitination: An Integrative Signaling Platform in Genome Stability. *Trends Genet.* 2021;37(6):566-81.
4. Ciechanover A. The ubiquitin–proteasome pathway: on protein death and cell life. *The EMBO Journal.* 1998;17(24):7151-60.
5. Hetz C, Zhang K, and Kaufman RJ. Mechanisms, regulation and functions of the unfolded protein response. *Nature Reviews Molecular Cell Biology.* 2020;21(8):421-38.
6. Hunt LC, Pagala V, Stephan A, Xie B, Kodali K, Kavdia K, et al. An adaptive stress response that confers cellular resilience to decreased ubiquitination. *Nature Communications.* 2023;14(1):7348.
7. Stewart MD, Ritterhoff T, Klevit RE, and Brzovic PS. E2 enzymes: more than just middle men. *Cell Research.* 2016;26(4):423-40.
8. Berndsen CE, and Wolberger C. New insights into ubiquitin E3 ligase mechanism. *Nature Structural & Molecular Biology.* 2014;21(4):301-7.
9. Jin J, Li X, Gygi SP, and Harper JW. Dual E1 activation systems for ubiquitin differentially regulate E2 enzyme charging. *Nature.* 2007;447(7148):1135-8.
10. Liu X, Zhao B, Sun L, Bhuripanyo K, Wang Y, Bi Y, et al. Orthogonal ubiquitin transfer identifies ubiquitination substrates under differential control by the two ubiquitin activating enzymes. *Nat Commun.* 2017;8:14286.
11. Ferrada MA, Savic S, Cardona DO, Collins JC, Alessi H, Gutierrez-Rodrigues F, et al. Translation of cytoplasmic UBA1 contributes to VEXAS syndrome pathogenesis. *Blood.* 2022;140(13):1496-506.
12. Lee PC, Dodart JC, Aron L, Finley LW, Bronson RT, Haigis MC, et al. Altered social behavior and neuronal development in mice lacking the Uba6-Use1 ubiquitin transfer system. *Mol Cell.* 2013;50(2):172-84.
13. Amer-Sarsour F, Falik D, Berdichevsky Y, Kordonsky A, Eid S, Rabinski T, et al. Disease-associated polyalanine expansion mutations impair UBA6-dependent ubiquitination. *Embo j.* 2024;43(2):250-76.
14. Collins JC, Magaziner SJ, English M, Hassan B, Chen X, Balanda N, et al. Shared and distinct mechanisms of UBA1 inactivation across different diseases. *Embo j.* 2024.
15. Lambert-Smith IA, Saunders DN, and Yerbury JJ. The pivotal role of ubiquitin-activating enzyme E1 (UBA1) in neuronal health and neurodegeneration. *Int J Biochem Cell Biol.* 2020;123:105746.
16. Ramser J, Ahearn ME, Lenski C, Yariz KO, Hellebrand H, von Rhein M, et al. Rare missense and synonymous variants in UBE1 are associated with X-linked infantile spinal muscular atrophy. *Am J Hum Genet.* 2008;82(1):188-93.
17. Beck DB, Ferrada MA, Sikora KA, Ombrello AK, Collins JC, Pei W, et al. Somatic Mutations in UBA1 and Severe Adult-Onset Autoinflammatory Disease. *New England Journal of Medicine.* 2020;383(27):2628-38.
18. Corty RW, Brogan J, Byram K, Springer J, Grayson PC, and Bick AG. VEXAS-Defining UBA1 Somatic Variants in 245,368 Diverse Individuals in the NIH All Of Us Cohort. *Arthritis*

Rheumatol. 2024.
19. Arlet J-B, Terrier B, and Kosmider O. Mutant UBA1 and Severe Adult-Onset Autoinflammatory Disease. *New England Journal of Medicine.* 2021;384(22):2163-5.
20. Grayson PC, Patel BA, and Young NS. VEXAS syndrome. *Blood.* 2021;137(26):3591-4.
21. Gurnari C, Pagliuca S, Durkin L, Terkawi L, Awada H, Kongkiatkamon S, et al. Vacuolization of hematopoietic precursors: an enigma with multiple etiologies. *Blood.* 2021;137(26):3685-9.
22. Obiorah IE, Patel BA, Groarke EM, Wang W, Trick M, Ombrello AK, et al. Benign and malignant hematologic manifestations in patients with VEXAS syndrome due to somatic mutations in UBA1. *Blood Adv.* 2021;5(16):3203-15.
23. Poulter J, Morgan A, Cargo C, and Savic S. A High-Throughput Amplicon Screen for Somatic UBA1 Variants in Cytopenic and Giant Cell Arteritis Cohorts. *J Clin Immunol.* 2022;42(5):947-51.
24. Li P, Venkatachalam S, Ospina Cordona D, Wilson L, Kovacsovics T, Moser KA, et al. A clinical, histopathological, and molecular study of two cases of VEXAS syndrome without a definitive myeloid neoplasm. *Blood Adv.* 2022;6(2):405-9.
25. Poulter JA, Collins JC, Cargo C, De Tute RM, Evans P, Ospina Cardona D, et al. Novel somatic mutations in UBA1 as a cause of VEXAS syndrome. *Blood.* 2021;137(26):3676-81.
26. Beck DB, Bodian DL, Shah V, Mirshahi UL, Kim J, Ding Y, et al. Estimated Prevalence and Clinical Manifestations of UBA1 Variants Associated With VEXAS Syndrome in a Clinical Population. *Jama.* 2023;329(4):318-24.
27. Mascaro JM, Rodriguez-Pinto I, Poza G, Mensa-Vilaro A, Fernandez-Martin J, Caminal-Montero L, et al. Spanish cohort of VEXAS syndrome: clinical manifestations, outcome of treatments and novel evidences about UBA1 mosaicism. *Ann Rheum Dis.* 2023;82(12):1594-605.
28. Sakuma M, Blombery P, Meggendorfer M, Haferlach C, Lindauer M, Martens UM, et al. Novel causative variants of VEXAS in UBA1 detected through whole genome transcriptome sequencing in a large cohort of hematological malignancies. *Leukemia.* 2023;37(5):1080-91.
29. Gurnari C, Pascale MR, Vitale A, Diral E, Tomelleri A, Galossi E, et al. Diagnostic capabilities, clinical features, and longitudinal UBA1 clonal dynamics of a nationwide VEXAS cohort. *Am J Hematol.* 2024;99(2):254-62.
30. Khitri M-Y, Hadjadj J, Mekinian A, and Jachiet V. VEXAS syndrome: An update. *Joint Bone Spine.* 2024;91(4):105700.
31. Koster MJ, Lasho TL, Olteanu H, Reichard KK, Mangaonkar A, Warrington KJ, et al. VEXAS syndrome: Clinical, hematologic features and a practical approach to diagnosis and management. *American Journal of Hematology.* 2024;99(2):284-99.
32. Padureanu V, Marinaș CM, Bobirca A, Padureanu R, Patrascu S, Dascalu AM, et al. Clinical Manifestations in Vacuoles, E1 Enzyme, X-Linked, Autoinflammatory, Somatic (VEXAS) Syndrome: A Narrative Review. *Cureus.* 2024;16(1):e53041.
33. de Valence B, Delaune M, Nguyen Y, Jachiet V, Heiblig M, Jean A, et al. Serious infections in patients with VEXAS syndrome: data from the French VEXAS registry. *Ann Rheum Dis.* 2024;83(3):372-81.
34. Chiaramida A, Obwar SG, Nordstrom AEH, Ericsson M, Saldanha A, Ivanova EV, et al. Sensitivity to targeted UBA1 inhibition in a myeloid cell line model of VEXAS syndrome. *Blood Adv.* 2023;7(24):7445-56.
35. Molteni R, Fiumara M, Campochiaro C, Tomelleri A, Diral E, Varesi A, et al. Unraveling Pathophysiology and Hematopoiesis of Vexas Syndrome By Multi-Omics Analyses and Targeted

Gene Editing. *Blood.* 2023;142(Supplement 1):2692-.
36. Stadtfeld M, and Graf T. Assessing the role of hematopoietic plasticity for endothelial and hepatocyte development by non-invasive lineage tracing. *Development.* 2005;132(1):203-13.
37. Kühn R, Schwenk F, Aguet M, and Rajewsky K. Inducible gene targeting in mice. *Science.* 1995;269(5229):1427-9.
38. Ventura A, Kirsch DG, McLaughlin ME, Tuveson DA, Grimm J, Lintault L, et al. Restoration of p53 function leads to tumour regression in vivo. *Nature.* 2007;445(7128):661-5.
39. Lee PP, Fitzpatrick DR, Beard C, Jessup HK, Lehar S, Makar KW, et al. A critical role for Dnmt1 and DNA methylation in T cell development, function, and survival. *Immunity.* 2001;15(5):763-74.
40. Rickert RC, Roes J, and Rajewsky K. B lymphocyte-specific, Cre-mediated mutagenesis in mice. *Nucleic Acids Res.* 1997;25(6):1317-8.
41. Tiedt R, Schomber T, Hao-Shen H, and Skoda RC. Pf4-Cre transgenic mice allow the generation of lineage-restricted gene knockouts for studying megakaryocyte and platelet function in vivo. *Blood.* 2007;109(4):1503-6.
42. Clausen BE, Burkhardt C, Reith W, Renkawitz R, and Förster I. Conditional gene targeting in macrophages and granulocytes using LysMcre mice. *Transgenic Res.* 1999;8(4):265-77.
43. Yona S, Kim KW, Wolf Y, Mildner A, Varol D, Breker M, et al. Fate mapping reveals origins and dynamics of monocytes and tissue macrophages under homeostasis. *Immunity.* 2013;38(1):79-91.
44. Muzumdar MD, Tasic B, Miyamichi K, Li L, and Luo L. A global double-fluorescent Cre reporter mouse. *Genesis.* 2007;45(9):593-605.
45. Passegué E, Wagner EF, and Weissman IL. JunB deficiency leads to a myeloproliferative disorder arising from hematopoietic stem cells. *Cell.* 2004;119(3):431-43.
46. Gutierrez-Rodrigues F, Kusne Y, Fernandez J, Lasho T, Shalhoub R, Ma X, et al. Spectrum of clonal hematopoiesis in VEXAS syndrome. *Blood.* 2023;142(3):244-59.
47. Ng MSF, Kwok I, Tan L, Shi C, Cerezo-Wallis D, Tan Y, et al. Deterministic reprogramming of neutrophils within tumors. *Science.* 2024;383(6679):eadf6493.
48. Wang Y, Wang J, Zheng W, Zhang J, Wang J, Jin T, et al. Identification of an IL-1 receptor mutation driving autoinflammation directs IL-1-targeted drug design. *Immunity.* 2023;56(7):1485-501.e7.
49. Cai Z, Aguilera F, Ramdas B, Daulatabad SV, Srivastava R, Kotzin JJ, et al. Targeting Bim via a lncRNA Morrbid Regulates the Survival of Preleukemic and Leukemic Cells. *Cell Rep.* 2020;31(12):107816.
50. Cai Z, Kotzin JJ, Ramdas B, Chen S, Nelanuthala S, Palam LR, et al. Inhibition of Inflammatory Signaling in Tet2 Mutant Preleukemic Cells Mitigates Stress-Induced Abnormalities and Clonal Hematopoiesis. *Cell Stem Cell.* 2018;23(6):833-49.e5.
51. Cai Z, Lu X, Zhang C, Nelanuthala S, Aguilera F, Hadley A, et al. Hyperglycemia cooperates with Tet2 heterozygosity to induce leukemia driven by proinflammatory cytokine-induced lncRNA Morrbid. *J Clin Invest.* 2021;131(1).
52. Cai Z, Zhang C, Kotzin JJ, Williams A, Henao-Mejia J, and Kapur R. Role of lncRNA Morrbid in PTPN11(Shp2)E76K-driven juvenile myelomonocytic leukemia. *Blood Adv.* 2020;4(14):3246-51.
53. Kosmider O, Possémé C, Templé M, Corneau A, Carbone F, Duroyon E, et al. VEXAS syndrome is characterized by inflammasome activation and monocyte dysregulation. *Nat Commun.*

2024;15(1):910.
54. Mizumaki H, Gao S, Wu Z, Gutierrez-Rodrigues F, Bissa M, Feng X, et al. In depth transcriptomic profiling defines a landscape of dysfunctional immune responses in patients with VEXAS syndrome. *Nat Commun.* 2025;16(1):4690.
55. He H, Wen Y, Huo Q, Yu H, Liu J, Jin W, et al. Cooperative progression of colitis and leukemia modulated by clonal hematopoiesis via PTX3/IL-1β pro-inflammatory signaling. *Genes & Diseases.* 2024:101397.
56. Boyadzhieva Z, Ruffer N, Kötter I, and Krusche M. How to treat VEXAS syndrome: a systematic review on effectiveness and safety of current treatment strategies. *Rheumatology (Oxford).* 2023;62(11):3518-25.
57. Salehi T, Callisto A, Beecher MB, and Hissaria P. Tofacitinib as a biologic response modifier in VEXAS syndrome: A case series. *Int J Rheum Dis.* 2023;26(11):2340-3.
58. Yu H, Zhang G, Ma Y, Ma T, Wang S, Ding J, et al. Single-cell and spatial transcriptomics reveal the pathogenesis of chronic granulomatous disease in a natural model. *Cell Rep.* 2025;44(5):115612.
59. Huo Q, Ding J, Zhou H, Wang Y, Wang S, He H, et al. Disruption of Morrbid alleviates autoinflammatory osteomyelitis in Pstpip2-deficient mice. *Dis Model Mech.* 2025.
60. Zhang G, Yu H, Liu J, Dong G, and Cai Z. Myeloid-lineage-specific membrane protein LRRC25 suppresses immunity in solid tumor and is a potential cancer immunotherapy checkpoint target. *Cell Rep.* 2025;44(5):115631.
61. Molteni R, Fiumara M, Campochiaro C, Alfieri R, Pacini G, Licari E, et al. Mechanisms of hematopoietic clonal dominance in VEXAS syndrome. *Nat Med.* 2025;31(6):1911-24.

LEGENDS for Figure 1 to Figure 13

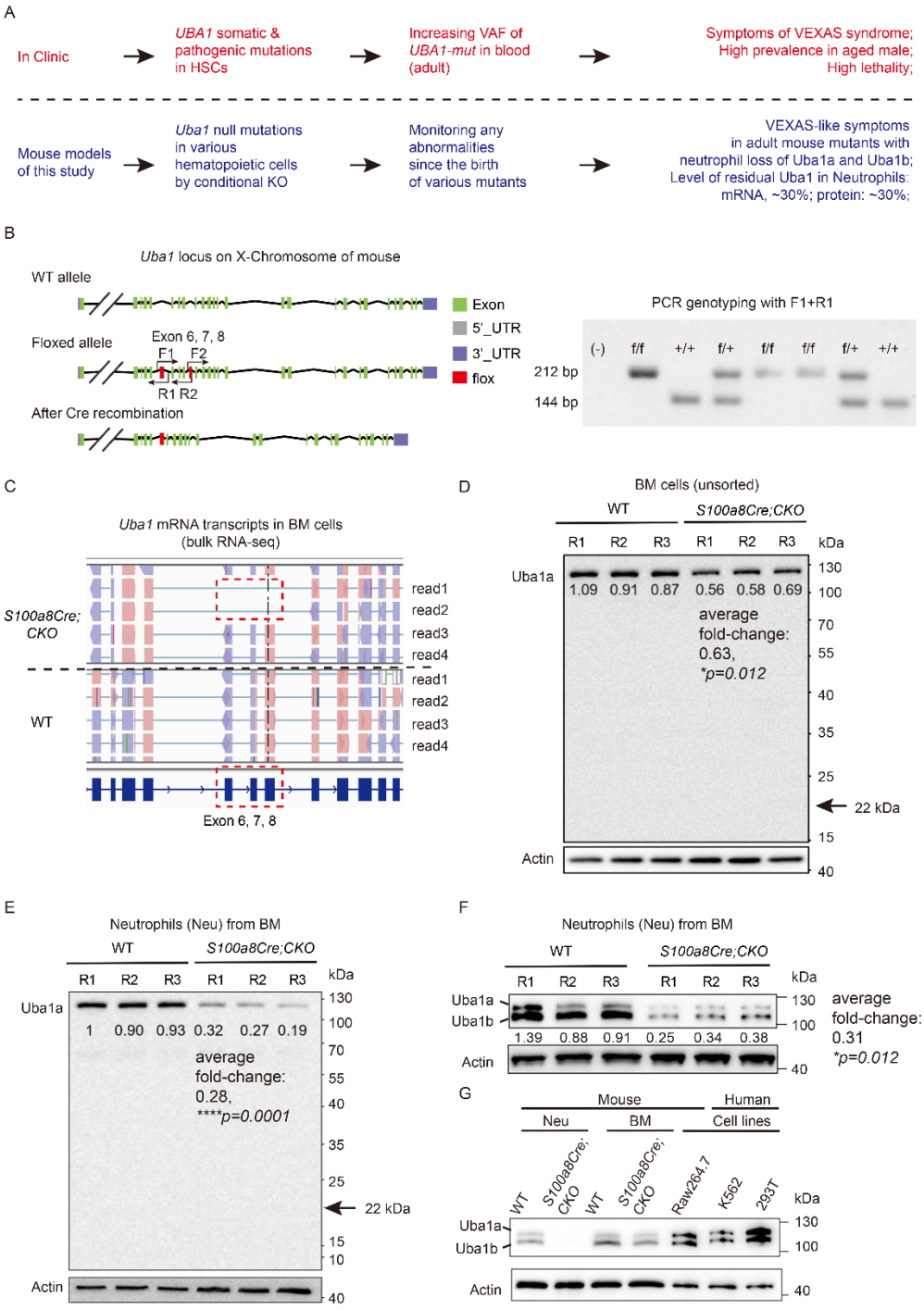

Figure 1: Conditional depletion of Uba1 in mice.

(A) A brief introduction of VEXAS syndrome occurrence in clinic and in the present study using CKO mouse models. CKO, conditional knock-out; HSC, hematopoietic stem cell; VAF, variant allele fraction.

(B) Gene structure of *Uba1* in mice and the CKO strategy in the present study. Mouse *Uba1* locus is in X-chromosome as human *UBA1*. Left panel: gene structure of

Uba1 in WT allele and the flox knock-in allele; Right panel: primers F1/R1 were used to distinguish WT and flox allele in the PCR genotyping.

(C) Disruption of *Uba1* transcripts was revealed by sequencing-read alignment in the bulk RNA-seq datasets of BM cells. The *S100a8Cre;CKO* mice used here for transcriptional chimerism analysis. BM, bone marrow.

(D) Expression of Uba1 protein in total BM cells by an antibody specific to Uba1a isoform. Note that no truncated Uba1a protein is detected (arrow marks the predicted molecular weight of putative truncated isoform, 22kDa). Three biological repeats (R1, R2 and R3) were used for WT and CKO mice.

(E) Expression of Uba1 isoform in purified neutrophil cells by the Uba1a-specific antibody. Note that the residual level of Uba1a in the isolated neutrophils of *S100a8Cre;CKO* is about 28% of that in WT controls (p=0.0001). Again, no truncated Uba1a protein is detected (arrow, 22kDa).

(F) Neutrophil depletion of Uba1a and Uba1b isoforms determined by an alternative antibody sensitive to the two Uba1 isoforms. Note that the residual level of Uba1 (two isoforms in total) in *S100a8Cre;CKO* is about 31% of that in WT controls (p=0.012).

(G) Expression of the two Uba1 isoforms (Uba1a and Uba1b) in primary BM cells of WT and *S100a8Cre;CKO*, in a mouse cell line Raw264.7, and in two human cell lines K562 and 293T.

*, p<0.05; ***, p<0.001; n=3~6 biological repeats. R1/R2/R3 indicates three independent biological repeats.

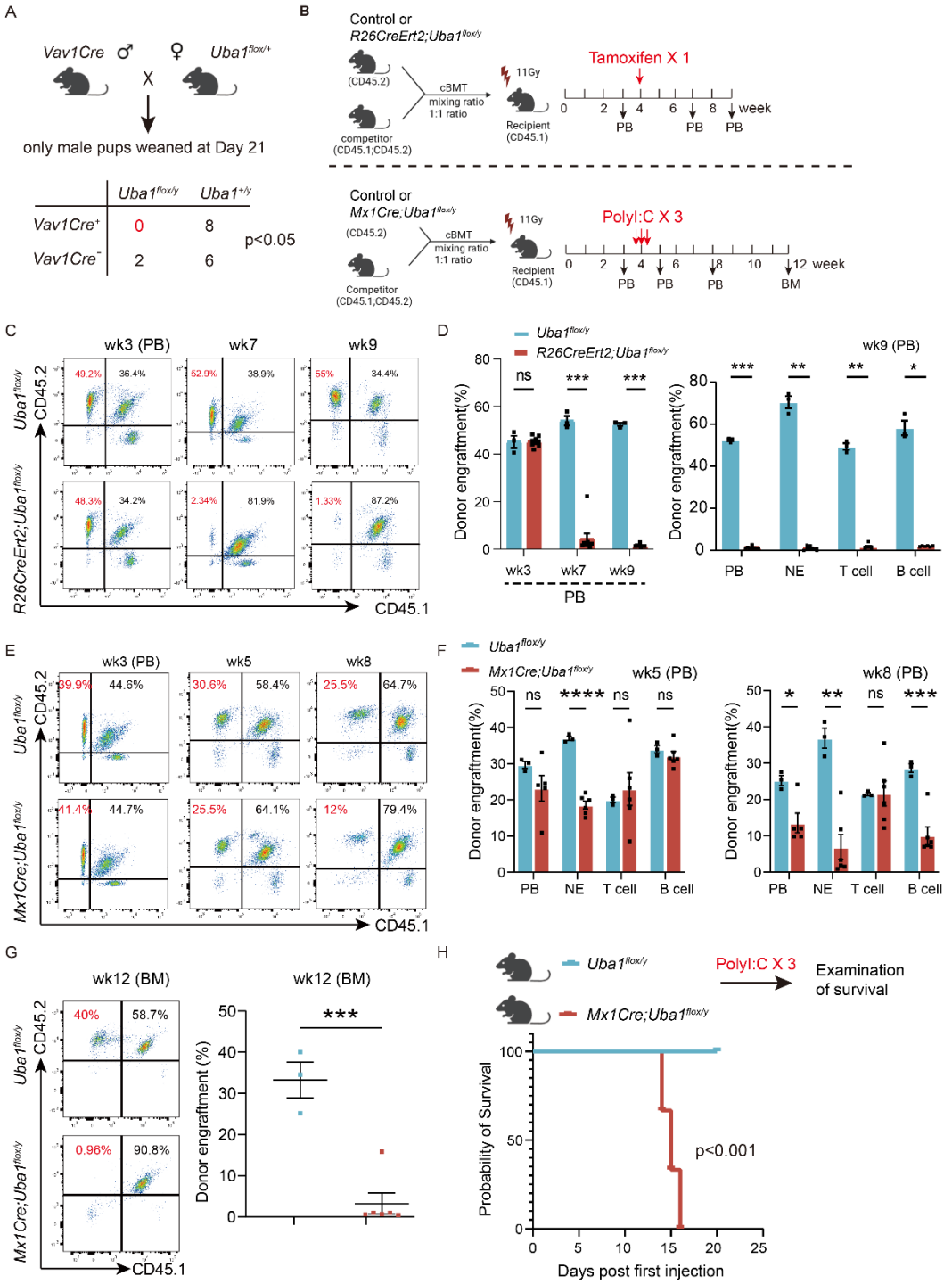

Figure 2: Conditional depletion of *Uba1* in hematopoietic stem cells (HSCs)

(A) Genetic crossing strategies for generating CKO mutants with depletion of *Uba1* in HSCs. *Vav1Cre*, *R26CreErt2* and *Mx1Cre* were used for this goal. In the scheme, the strategy for generation *Vav1Cre;Uba1$^{flox/y}$* is shown as an example (upper panel). No *Vav1Cre;Uba1$^{flox/y}$* male pups were observed, suggesting lethality of *Vav1Cre*-mediated depletion of Uba1 in the HSCs at the embryonic stages (lower panel; chi-square test, $p<0.05$)

(B) Generation of chimeric mice with depletion of Uba1 in 50% of HSCs. The chimeric mice with BM reconstituted by cBMT assays through mixing *R26CreErt2;Uba1$^{flox/y}$* or *Mx1Cre;Uba1$^{flox/y}$* donors (CD45.2^{+}) with competitor donors (F1 mice:

CD45.1$^+$CD45.2$^+$) as indicated (mixing ratio, 1:1). The recipient mice were CD45.1$^+$. Induced depletion of *Uba1* in *R26CreErt2;Uba1$^{flox/y}$* chimeric mice was conducted by feeding with tamoxifen (one dose post cBMT). The induced depletion of *Uba1* in *Mx1Cre; Uba1$^{flox/y}$* chimeric mice was conducted by i.p. injection of PolyI:C (three doses post cBMT). cBMT, competitive bone marrow transplant.

(**C-D**) Representative flow cytometry profiles and the quantification of the donor engraftment in the *R26CreErt2;Uba1$^{flox/y}$* chimeric mice at the indicated time points. n=3~5 chimeric animals per group.

(**E-G**) Representative flow cytometry profiles and the quantification of the donor engraftment in the *Mx1Cre;Uba1$^{flox/y}$* chimeric mice at the indicated time points. **E** and **F** are results from flow cytometry analysis on peripheral blood cells (PB) while **G** is result from flow cytometry analysis on BM cells. n=3~6 animals per group.

(**H**) *Mx1Cre;Uba1$^{flox/y}$* primary mice proceeded to a quick death within 20 days after induction with PolyI:C (3 doses). Age of the mice, 8~12 weeks old. n=5 animals per group.

ns, not significant; *, p<0.05; **, p<0.01; ***, p<0.001; ****, p<0.0001; n=3~6 biological repeats.

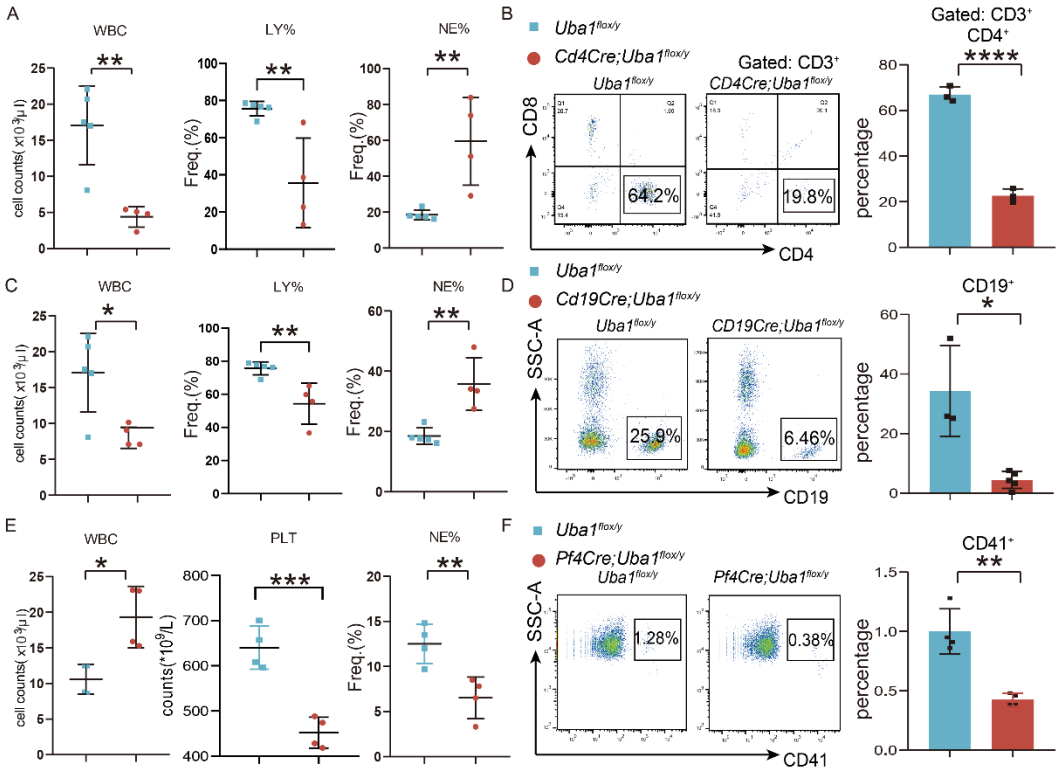

Figure 3: Conditional depletion of *Uba1* in CD4$^+$T cells, CD19$^+$B cells, and megakaryocytes

(**A-D**) Loss of *Uba1* in lymphoid cells (*Cd4Cre*- or *Cd19Cre*-induced) results in obviously decreased number of leukocytes in PB. **A** and **B**, results from *Cd4Cre; Uba1$^{flox/y}$* primary male mice; **C** and **D**, results from *Cd19Cre;Uba1$^{flox/y}$* primary male mice. **A** and **C**, analysis of blood cells by the hematological analyzer; **B** and **D**, representative flow cytometry profiles and quantification of the flow cytometry results. WBC, white blood cell; LY, lymphocyte; NE, neutrophil; PLT, platelet.

(**E-F**) Loss of *Uba1* in megakaryocytes (*Pf4Cre*-induced) results in decreased number of platelets and megakaryocytes in PB. **E**, analysis of blood cells by the hematological analyzer; **F**, representative flow cytometry profiles and quantification of the flow cytometry results.

*, p<0.05; **, p<0.01; ***, p<0.001; ****, p<0.0001; n=4~5 biological repeats.

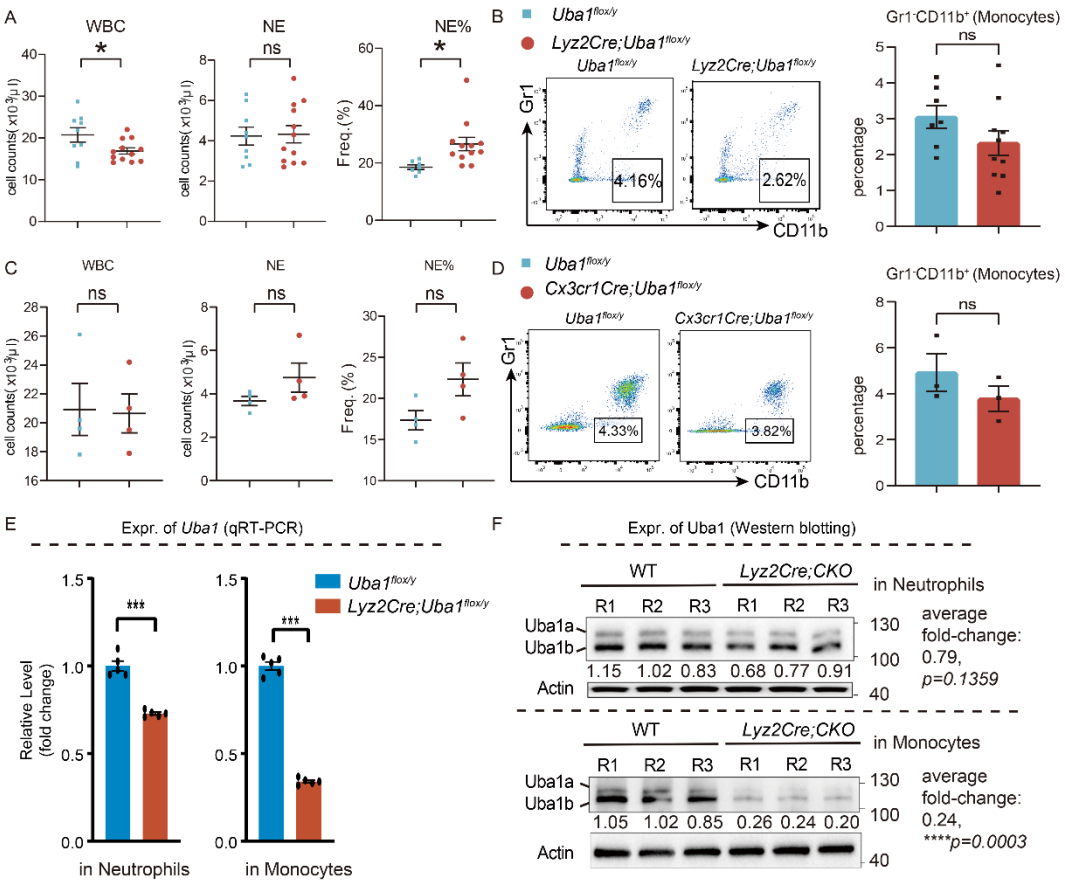

Figure 4: Conditional depletion of *Uba1* in monocytes and macrophages

(**A-D**) Mice with monocyte and macrophage-specific loss of *Uba1* remained viable and did not develop VEXAS-like symptoms. **A-B**, results from *Lyz2Cre;Uba1$^{flox/y}$* primary male mice; **C-D**, results from *Cx3cr1Cre;Uba1$^{flox/y}$* primary male mice. **A** and **C**, analysis of blood cells by the hematological analyzer; **B** and **D**, representative flow cytometry profiles and quantification of the flow cytometry results. Note *Lyz2Cre;Uba1$^{flox/y}$* CKO mutants manifested a subtle increased count of WBC and increased percentage of neutrophils.

(**E**) Quantification of residual *Uba1* mRNA transcripts in neutrophils and monocytes from WT (*Uba1$^{flox/y}$*) and *Lyz2Cre;CKO* (*Lyz2Cre;Uba1$^{flox/y}$*) by qRT-PCR assays. Compared to the controls, residual average level of *Uba1* mRNA transcripts in mutant neutrophils is about 75% while that in the mutant monocytes is 25% in *Lyz2Cre;Uba1$^{flox/y}$* CKO, suggesting *Lyz2Cre* is mainly active in monocytes and with subtle leakage in neutrophils. n=5 biological repeats.

(**F**) Quantification of residual Uba1 proteins in neutrophils and monocytes from WT (*Uba1$^{flox/y}$*) and *Lyz2Cre;CKO* (*Lyz2Cre;Uba1$^{flox/y}$*) by western blotting assays. Upper panel, expression of Uba1 in isolated neutrophils. Lower panel, expression of Uba1 in isolated monocytes. Note that in the *Lyz2Cre;CKO* mutants, 76% reduction of Uba1 was detected in monocytes (average residual level: 24%, p = 0.0003) while only 21% reduction of Uba1 in neutrophils (average residual level: 79%, p = 0.1359) were detected. Three independent biological repeats were included (R1, R2 and R3).

ns, not significant; *, p<0.05; **, p<0.01; ***, p<0.001; ****, p<0.0001; n=3~11 biological repeats.

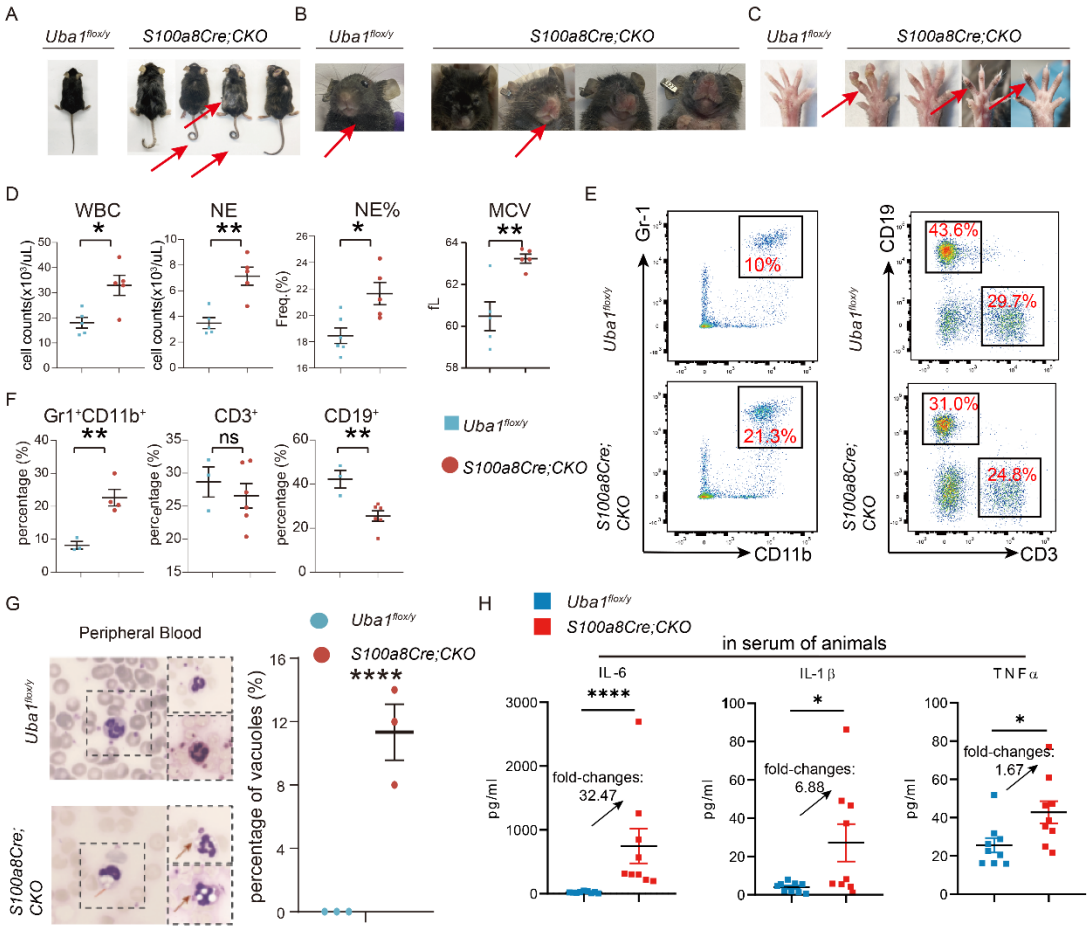

Figure 5: VEXAS-like autoinflammatory symptoms in *S100a8Cre;CKO* mice.

(**A**) *S100a8Cre;CKO* mice manifested obvious dermatitis and hair loss on their back (penetration rate: 100%; n=20).

(**B**) *S100a8Cre;CKO* mice manifested flare noses (penetration rate: 100%; n=20).

(**C**) *S100a8Cre;CKO* mice manifested swollen paw (penetration rate: ~50%; n=20) and their knuckles of paws were pigmented (penetration rate: 100%; n=20). In **A** to **C**, the penetration rate for checking the phenotypes were calculated at the age about 6~12-month-old. Stronger phenotypes and greater penetration rates were determined in aged mutant mice.

(**D**) Aberrant hematological parameters in peripheral blood (PB) of *S100a8Cre;CKO* mutants. WBC, white blood cell; NE, neutrophil; MCV, mean corpuscular volume.

(**E-F**) Representative flow cytometry profiles of PB and quantifications of mature neutrophils ($Gr1^+CD11b^+$) and lymphoid cells ($CD3^+$ or $CD19^+$).

(**G**) About 10% of vacuolized neutrophils were identified in the *S100a8Cre;CKO* mice. Giemsa staining and bright-light microscopy were performed on the blood samples.

(**H**) Serum levels of pro-inflammatory cytokines IL-6, IL-1β, and TNFα were upregulated in the VEXAS-like mutant *S100a8Cre;CKO* mice. These cytokines were part of a 10-cytokine panel. See the full profiles in **Figure S7A**.

ns, not significant; *, $p<0.05$; **, $p<0.01$; ***, $p<0.001$; ****, $p<0.0001$; n=3~20 biological repeats.

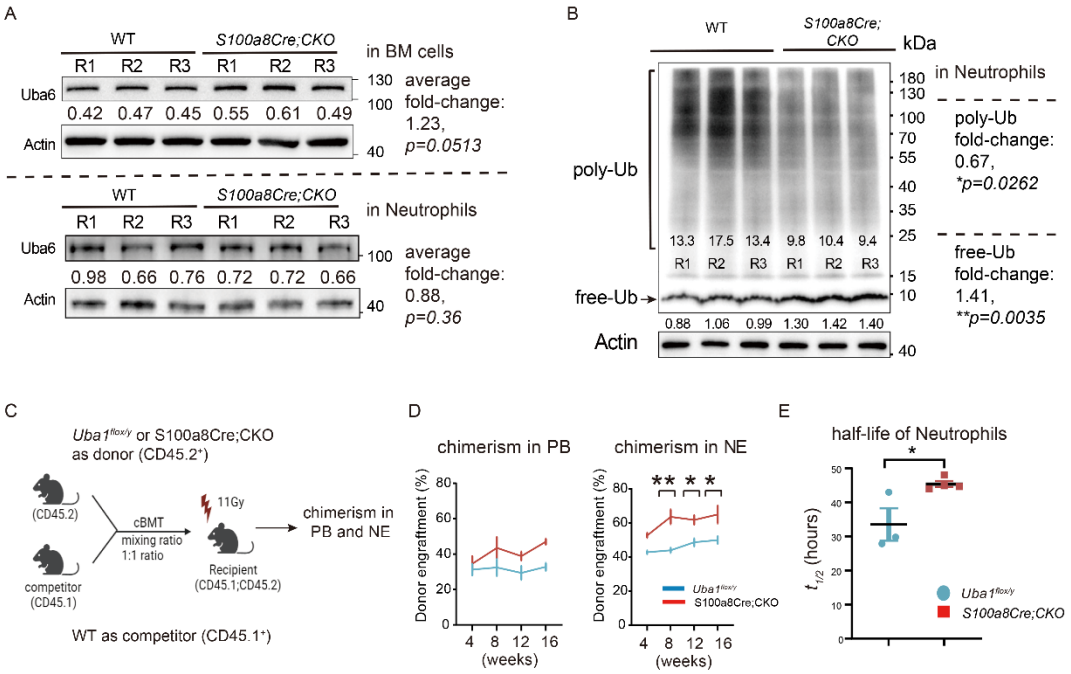

Figure 6: Ubiquitylation and cell survival in the *S100a8Cre;CKO* neutrophils

(**A**) Expression of another E1 enzyme Uba6 appeared grossly normal in total BM cells (upper panel) and isolated neutrophils (lower panel) of the *S100a8Cre;CKO* mice. R1/R2/R3 indicates three independent biological repeats.

(**B**) Poly-ubiquitin (poly-Ub) and free ubiquitin (free-Ub) levels were quantified by western blotting in isolated neutrophils of the WT and *S100a8Cre;CKO*. Decreased poly-Ub and increased free-Ub levels were determined in the *S100a8Cre;CKO* mice by the assays. R1/R2/R3 indicates three independent biological repeats.

(**C-D**) Comparing the growth and survival advantage of WT-neutrophils and mutant-neutrophils by cBMT assays. BM cells from *S100a8Cre;CKO* and WT donors were isolated for performing the cBMT assays. **C**, the scheme for the cBMT experimental procedures. **D**, chimerism analysis in PB samples or in isolated neutrophils at the indicated time points post the cBMT.

(**E**) Measuring the half-life ($t_{1/2}$) of neutrophils in the peripheral blood by BrdU pulse assays. See **Methods** for details about the full experimental procedures of BrdU staining, flow cytometry and computational analysis.

*, $p<0.05$; **, $p<0.01$; n=3~5 biological repeats for **A-D**. n=3~4 BrdU chasing assays for **E** and each chasing assay used 6 biological repeats.

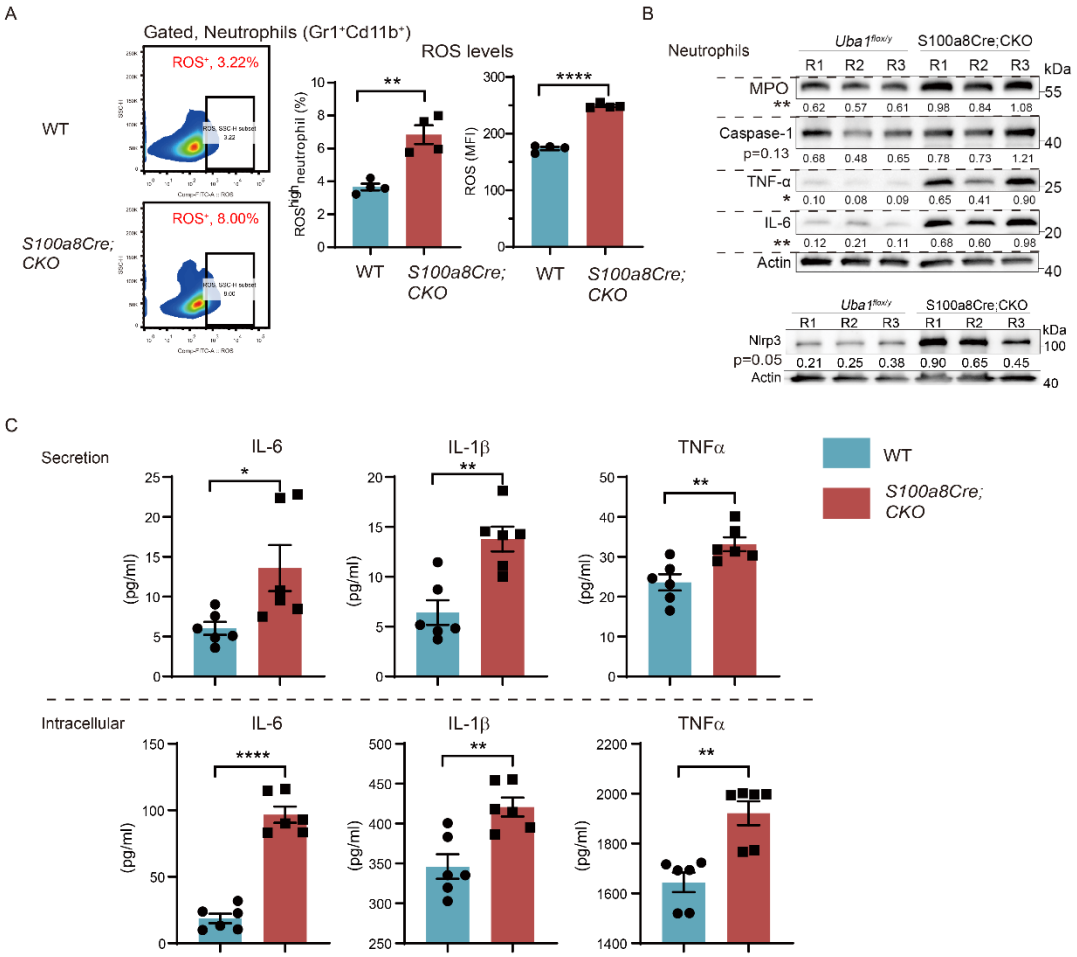

Figure 7: Cell-autonomous pro-inflammatory activation in the *S100a8Cre;CKO* neutrophils.

(A) Measuring ROS production in neutrophils by flow cytometry. Neutrophils from BM were gated by $Gr1^{+}Cd11b^{+}$ staining before the ROS analysis. Left panel, representative flow cytometry profiles. Right panel, the quantitative results of ROS^{high} neutrophils and ROS expression level. MFI, mean fluorescence intensity. n = 4 biological repeats per group.

(B) Western blotting analysis on inflammatory markers as indicated. Myeloperoxidase (MPO) is a classic readout of inflammation; IL-6 and TNFα are proinflammatory cytokines; Nlrp3 and Caspase-1 are important components of inflammasome complex or pathways. The fold changes of the tested proteins are between the ranges of 1.5 (Caspase-1) and 7.25 (TNFα). *P* values were labeled for each marker on the panel. R1/R2/R3 indicates three independent biological repeats.

(C) Secretion and intracellular level of the proinflammatory cytokines measured by ELISA. To measure the secretion level, 1 x 10^6 purified neutrophils were cultured for 24 hours in the 96-well plate with 100 μL medium. To measure the intracellular level, 1 x 10^7 purified neutrophils were incubated with RIPA lysis buffer. n = 4~6 biological repeats per group.

*, $p<0.05$; **, $p<0.01$; ***, $p<0.001$; ****, $p<0.0001$; n=3~6 biological repeats.

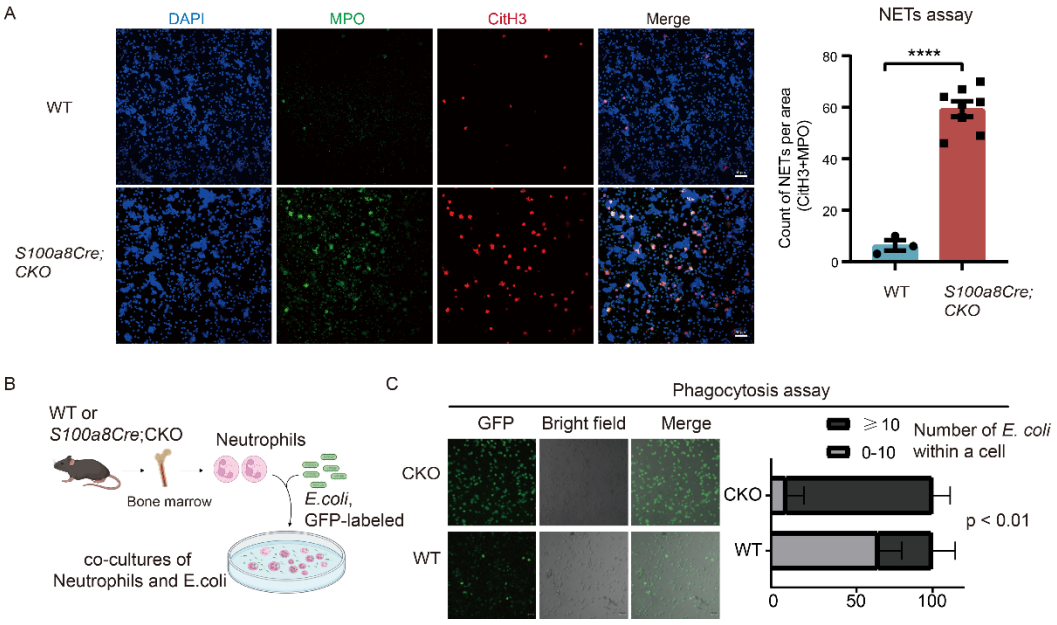

Figure 8: NETs formation and phagocytosis in the *S100a8Cre;CKO* neutrophils

(A) Mutant neutrophils manifested increased level of NETs formation. NETs formation was determined by MPO and CitH3 staining. 1 x 10^6 purified neutrophils were cultured in the 24-well plate with 1000 µL medium. PMA was added to the medium to promote cell attachment. After 6-hour culture, cells were fixed and stained by MPO and CitH3 antibody. MPO and CitH3 double-positive cells were count for a standard area. Left panel, representative microscopy images; right panel, quantification results. n = 3 biological repeats for WT group and 8 biological repeats for *S100a8Cre;CKO* group.

(**B-C**) Mutant neutrophils manifested increased phagocytosis capability when co-cultured with bacteria *E.coli* (GFP^+). **B**, Scheme for phagocytosis assay. Time-lapse photography was performed every 10 minutes post the mixing. GFP dots (indication of *E.coli*) within the neutrophils were counted at the time point 40 minutes post the mixing of neutrophils and bacteria **C**, Phagocytosis of *E.coli* was improved in *S100a8Cre;CKO* neutrophils compared to WT. Data are presented as the percentages of cells with certain counts of internalized bacteria (GFP^+). n=3 biological repeats per group.

**, p<0.01; ****, p<0.0001; n=3~8 biological repeats.

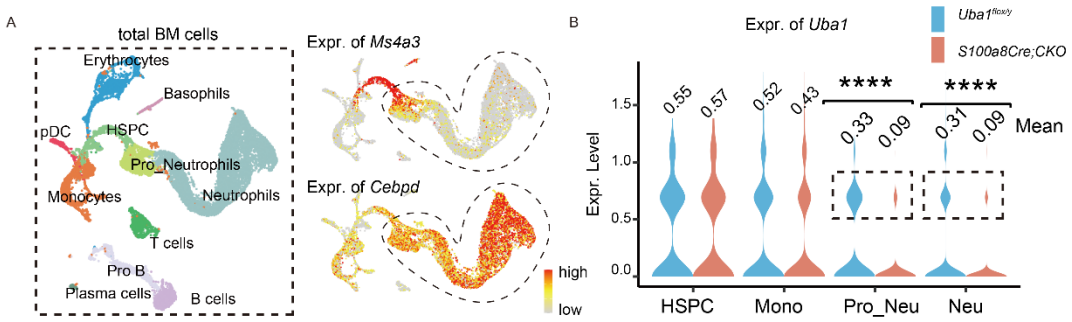

Figure 9: Neutrophil-specific depletion of *Uba1* in *S100a8Cre;CKO* revealed by the scRNA-seq analysis on the BM cells

(A) BM cells from *Uba1*$^{flox/y}$ (WT) and *S100a8Cre;CKO* mice were subject for single-cell RNA-sequencing (scRNA-seq) analysis. A total of 11 major hematopoietic cell types were annotated in the UMPA plot. Of note, two types of neutrophils are highlighted: Pro-Neutrophils and Neutrophils. As shown in the right panel, expression of *Ms4a3* (marker for granulocyte-macrophage progenitor [GMP] cells) and *Cebpd* (marker for primitive and mature neutrophils) marks the developmental continuity from HSPC/GMP to neutrophils. UMAP, Uniform Manifold Approximation and Projection for Dimension Reduction; HSPC, hematopoietic stem and progenitor cells.

(B) Expression of *Uba1* in HSPCs, Monocytes, Pro-Neutrophils and Neutrophils were quantified in *Uba1*$^{flox/y}$ (WT) and *S100a8Cre;CKO* scRNA-seq datasets. Note that there is no reduction of *Uba1* expression in HSPCs from the *S100a8Cre;CKO* (residual level: 104%), a slight decrease of *Uba1* in Monocytes (residual level: 82%) and a dramatic decrease of *Uba1* in Pro-Neutrophils or in Neutrophils (residual level: 27% and 29%, respectively).

Each single cell of the indicated cell types was included for the Uba1 expression analysis. ****, $p<0.0001$.

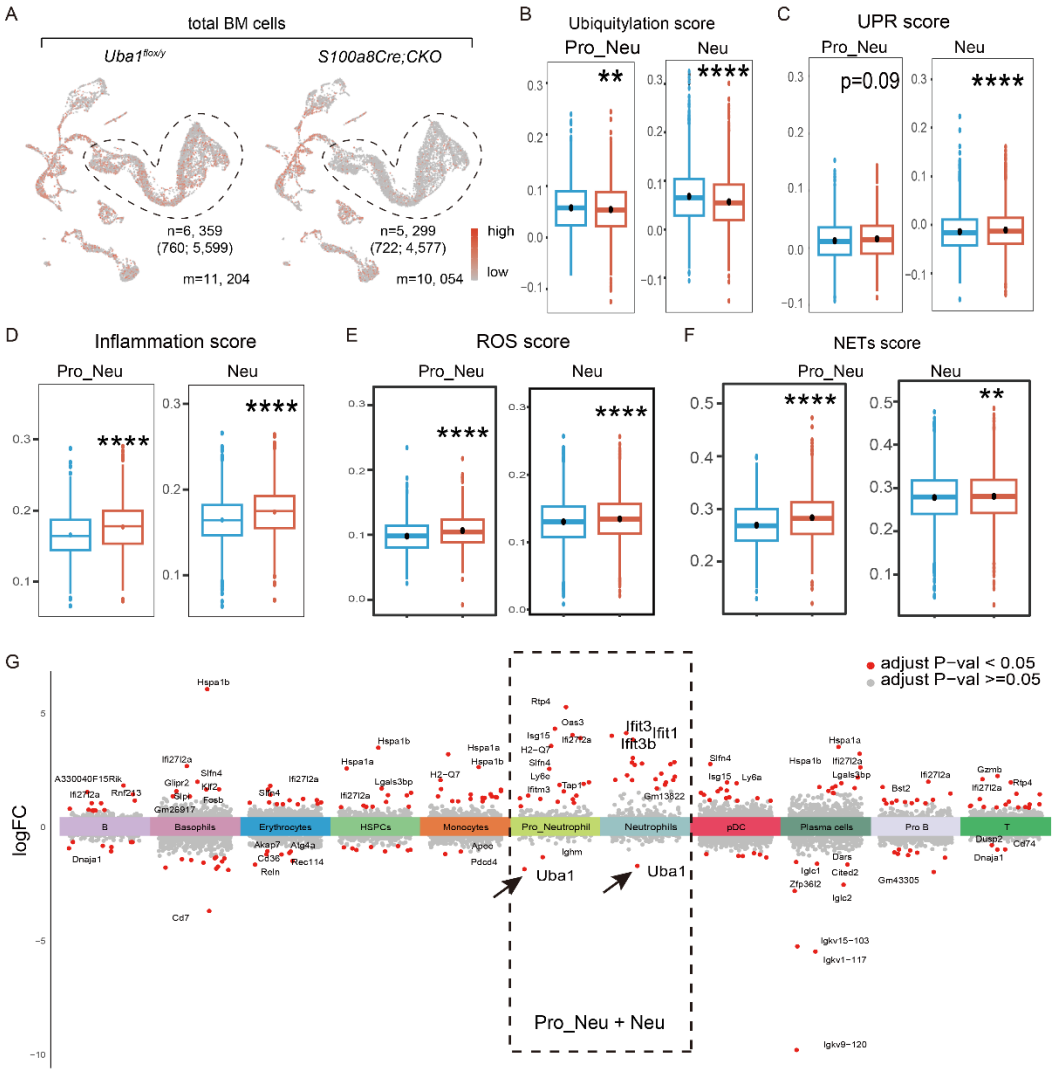

Figure 10: Disturbed neutrophils homeostasis revealed by single-cell computational analysis

(A) Pro-Neutrophils and Neutrophils were highlighted in the UMAP plot and for downstream analysis of cell homeostasis. For WT, 760 Pro-Neutrophils and 5,599 Neutrophils included in the downstream analysis; For *S100a8Cre;CKO*, 722 Pro-Neutrophils and 4,577 Neutrophils included in the downstream analysis.

(B) *S100a8Cre;CKO* mice manifested decreased ubiquitylation score in Pro-Neutrophils or in Neutrophils compared to WT. The result is expected as Uba1 is an E1 enzyme responsible for ubiquitin activation.

(**C-F**) Loss of *Uba1* in neutrophils resulted in disturbed cellular homeostasis as indicated by increased UPR Score (**C**), Inflammatory Score (**D**), ROS Score (**E**) and NETs Score (**F**). UPR, unfolded protein stress response; ROS, reactive oxygen species; NETs, neutrophils extracellular trap formation.

(G) Manhattan plots of differentially expressed genes (DEGs) in each indicated cell type. As highlighted in the dotted-line area, expression of *Uba1* is downregulated (arrows) and expression of certain pro-inflammatory genes (i.e. *Ifit1* and *Ifit3*) are upregulated in Pro_Neutrophils and Neutrophils from *S100a8Cre;CKO* mice compared with those from WT controls.

Each single cell of the indicated cell types was included for the cellular activity analysis. **, $p<0.01$; ****, $p<0.0001$.

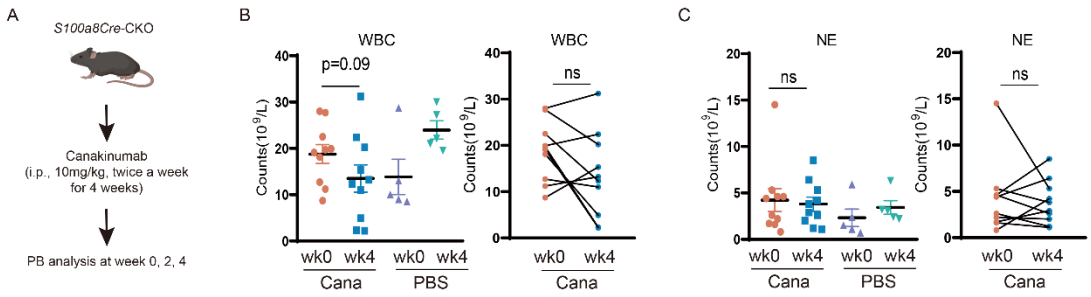

Figure 11: Intervention of the VEXAS-like symptoms by inhibition of IL-1β/IL-1R1

(**A**) *S100a8Cre;CKO* mice were subjected for treatment with Canakinumab (anti-IL1β). No pre-tests were performed and the regime of Canakinumab in mice was designed as 10 mg/kg, i.p., twice a week for 4 weeks.

(**B-C**) At the end-point of the drug treatment, we observed only reduction of WBC counts while the counts of neutrophils remained unchanged. MCV was also unchanged.

n=8 biological repeats per group. ns, not significant. See also **Figure S8** for the treatment with Anakinra (anti-IL1R1), which also only partially mitigate the VEXAS-like symptoms in the *S100a8Cre;CKO* mice.

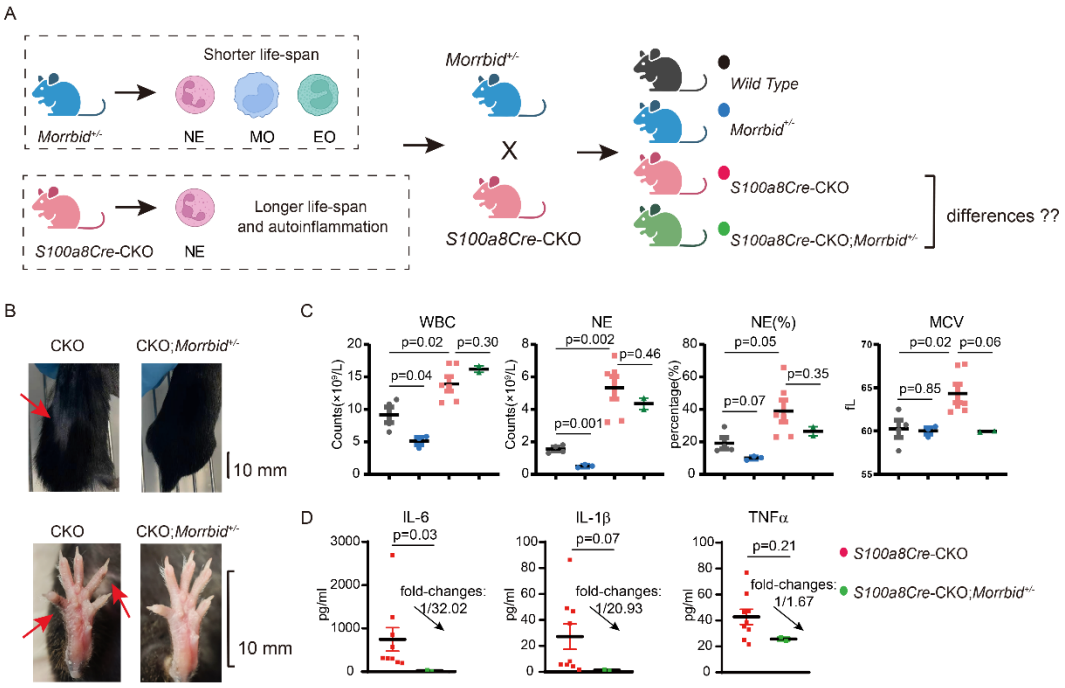

Figure 12: Intervention of the VEXAS-like symptoms by genetic loss of *Morrbid*

(**A**) *S100a8Cre;CKO* mice were bred with *Morrbid*$^{+/-}$ for testing the role of *Morrbid* in the autoinflammation disease VEXAS syndrome. The human-mouse conserved lncRNA gene *Morrbid* is a pro-survival regulator for myeloid cells, especially for neutrophils (NE), monocytes (Mo) and eosinophils (Eo). Similar to the homozygous *Morrbid*$^{-/-}$, the heterozygous mutant *Morrbid*$^{+/-}$ manifests similar shorter lifespan of the myeloid cells. We generated the compound mutants *S100a8CreCKO*;*Morrbid*$^{+/-}$ mice along with other controls to determine the role of *Morrbid* in VEXAS syndrome.

(**B**) Hair loss on the back and pigmentation on the paw knuckles were mitigated in the compound mutants *S100a8CreCKO;Morrbid*$^{+/-}$ mice.

(**C**) Hematological analysis on the peripheral blood cells. MCV, NE counts and NE percentage (NE%) all were with a decreased trend, indicating the mitigation of VEXAS-like symptoms by genetic loss of *Morrbid*. WBC, white blood cell; NE, neutrophil; MCV, mean corpuscular volume.

(**D**) Serum level of pro-inflammatory cytokines IL-6, IL-1β, and TNFα all were downregulated in the compound mutants *S100a8CreCKO*;*Morrbid*$^{+/-}$ mice.

Fold changes and *p* values are labeled in **C** and **D**. n=3~9 biological repeats per group.

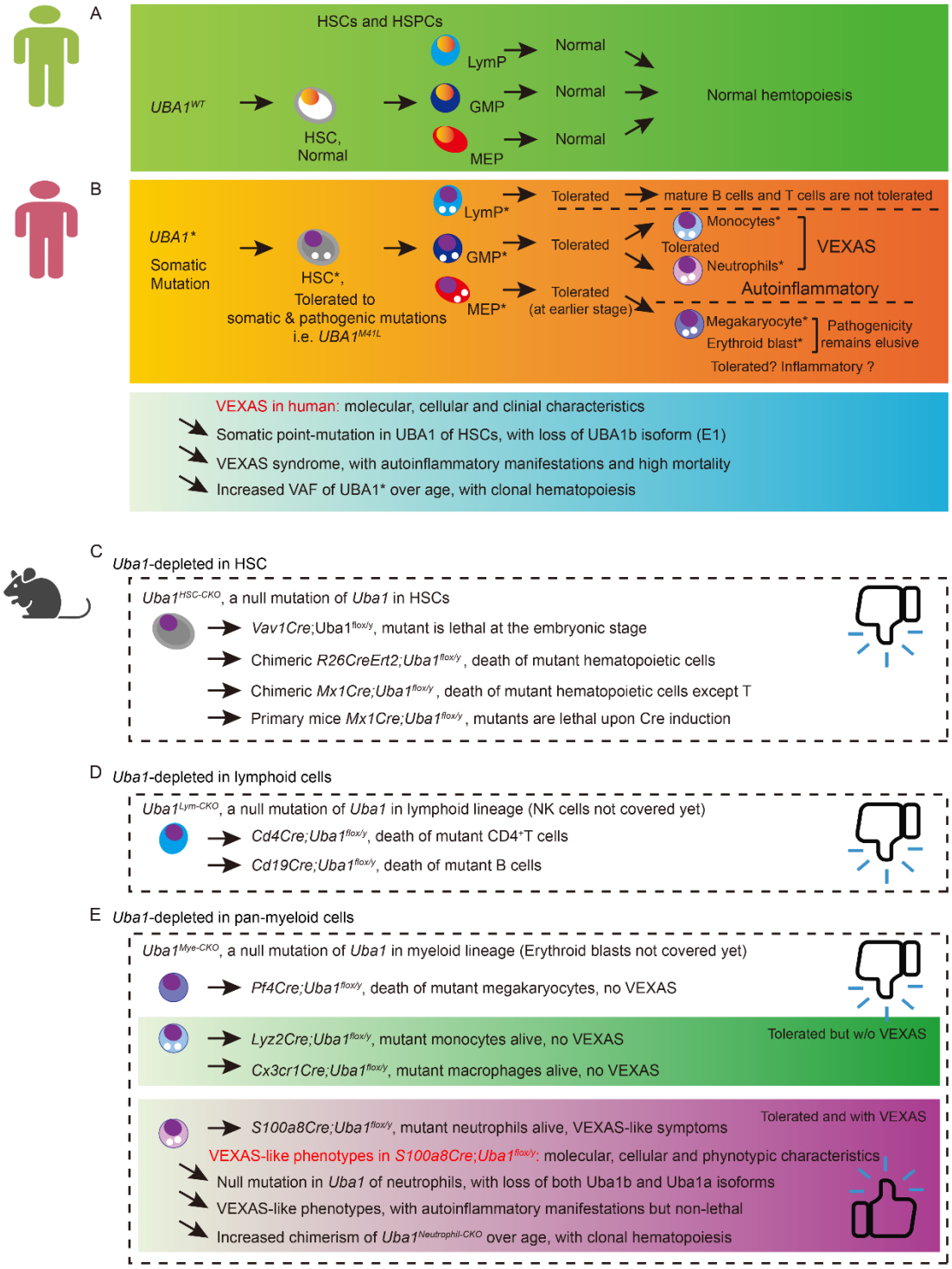

Figure 13: Summary of the study and a comparison with VEXAS-related clinical studies

(**A-B**) Normal and VEXAS-conditioned hematopoiesis are illustrated in **A** and **B** respectively. Additionally, according to the published clinical results, as summarized in lower panel of **B**, VEXAS patients manifest three typical features: 1. A somatic and pathogenic *UBA1* point-mutation in HSCs (typically at the M41 site, indicating a loss of the cytoplasm isoform UBA1b), and the VEXAS-related outcomes should be attributed to the combination effect of all blood cells; 2. Autoinflammatory symptoms at older ages (around 40-year-old to older for aged male); and 3. Increased variant allele

fraction (VAF) of mutant *UBA1* and occurrence of clonal hematopoiesis.
(**C**-**E**) The outcomes of 9 different CKO lines of the study are summarized in **C**, **D**, and **E** respectively. Except monocytes and neutrophils, we demonstrate that most of hematopoietic progenitor and mature cells are not tolerated to the null-version mutation of *Uba1.* Importantly, we demonstrate that monocyte and neutrophils survive with ~30% residual level of Uba1. However, monocyte depletion of Uba1 in *Lyz2Cre*;CKO and *Cx3cr1Cre*;CKO did not develop VEXAS-like symptoms as neutrophil depletion of Uba1 in *S100a8Cre*;CKO. As summarized in lower panel of **E**, VEXAS-like symptoms in *S100a8Cre*;CKO also include three typical features: 1. A null-version of mutation in *Uba1* of neutrophils, indicating both nucleic and cytoplasm isoforms are deficient and consequences are mainly attributed to mutant neutrophils; 2. Autoinflammatory symptoms are typically initiated at 4-month-old and extended to older ages (i.e. 6-month-old to older) but the life-span of the *S100a8Cre*;CKO mutant animals are grossly normal; and 3. Increased fraction of mutant neutrophils and occurrence of clonal hematopoiesis are indicated by the cBMT experiments.
See also Discussion in the Main text and **Table S1** to **S4** in the **Supplemental Material** for further comparisons through different angles.